
Theses and Dissertations

2010

Critical knots for minimum distance energy and complementary domains of arrangements of hypersurfaces

William George Hager
University of Iowa

Copyright 2010 William George Hager

This dissertation is available at Iowa Research Online: <http://ir.uiowa.edu/etd/679>

Recommended Citation

Hager, William George. "Critical knots for minimum distance energy and complementary domains of arrangements of hypersurfaces." PhD (Doctor of Philosophy) thesis, University of Iowa, 2010. <http://ir.uiowa.edu/etd/679>.

Follow this and additional works at: <http://ir.uiowa.edu/etd>

 Part of the [Mathematics Commons](#)

CRITICAL KNOTS FOR MINIMUM DISTANCE ENERGY AND
COMPLEMENTARY DOMAINS OF ARRANGEMENTS OF
HYPERSURFACES

by

William George Hager

An Abstract

Of a thesis submitted in partial fulfillment of the
requirements for the Doctor of Philosophy degree
in Mathematics in
the Graduate College of
The University of Iowa

July 2010

Thesis Supervisor: Professor Jonathan K. Simon

ABSTRACT

In this thesis, we will discuss two separate topics. First, we find a critical polygonal knot for a certain knot energy function. A knot is a closed curve or polygon in three space. It is possible to for a computer to simulate the flow of a knot to a minimal energy conformation. There is no guarantee, however, that a true minimizer exists near the computer's alleged minimizer. We take advantage of both the symmetry of the alleged minimizer and the symmetry invariance of the energy function to prove that there is a critical point of the energy function near the computer's minimizer.

Second, we will discuss how to determine the number of complementary domains of arrangements of algebraic curves in 2-space and ellipsoids in 3-space. In each of these situations, we supply equations that provide an upper bound for the number of complementary domains. These upper bounds are applicable even when the exact intersections between the curves or surfaces are unknown.

Abstract Approved: _____
Thesis Supervisor

Title and Department

Date

CRITICAL KNOTS FOR MINIMUM DISTANCE ENERGY AND
COMPLEMENTARY DOMAINS OF ARRANGEMENTS OF
HYPERSURFACES

by

William George Hager

A thesis submitted in partial fulfillment of the
requirements for the Doctor of Philosophy degree in Mathematics
in the Graduate College of
The University of Iowa

July 2010

Thesis Supervisor: Professor Jonathan K. Simon

Copyright by
WILLIAM GEORGE HAGER
2010
All Rights Reserved

Graduate College
The University of Iowa
Iowa City, Iowa

CERTIFICATE OF APPROVAL

PH.D. THESIS

This is to certify that the Ph.D. thesis of

William George Hager

has been approved by the Examining Committee
for the thesis requirement for the Doctor of
Philosophy degree in Mathematics at the July 2010
graduation.

Thesis Committee: _____
Jonathan Simon, Thesis Supervisor

Richard Randell

Oguz Durumeric

Walter Seaman

John Robinson

My heartfelt thanks to those
who have helped me along the way.

To my parents: You are my greatest teachers.
Words cannot express my gratitude.

To my wife: Thank you for your unending
support and occasional butt-kicking.

To my advisor: Thank you for your
constant pushing and insight.

To Dr. Randell: Thank you for spending so much of your
time trying to explain algebra to a topologist.

To Dr. Durumeric: Thank you for providing
much needed clarity.

ABSTRACT

In this thesis, we will discuss two separate topics. First, we find a critical polygonal knot for a certain knot energy function. A knot is a closed curve or polygon in three space. It is possible to for a computer to simulate the flow of a knot to a minimal energy conformation. There is no guarantee, however, that a true minimizer exists near the computer's alleged minimizer. We take advantage of both the symmetry of the alleged minimizer and the symmetry invariance of the energy function to prove that there is a critical point of the energy function near the computer's minimizer.

Second, we will discuss how to determine the number of complementary domains of arrangements of algebraic curves in 2-space and ellipsoids in 3-space. In each of these situations, we supply equations that provide an upper bound for the number of complementary domains. These upper bounds are applicable even when the exact intersections between the curves or surfaces are unknown.

TABLE OF CONTENTS

LIST OF FIGURES	vi
CHAPTER	
1 INTRODUCTION	1
1.1 Outline of Chapter 2	1
1.2 Outline of Chapter 3	2
1.3 Outline of Chapter 4	3
2 MINIMUM DISTANCE ENERGY FUNCTION MINIMIZERS	4
2.1 Basic Definitions	4
2.2 Understanding Six Segment Dihedral Knots	5
2.3 Definitions	8
2.4 The Minimum Distance Energy Function	10
2.5 Preview of Coming Attractions	14
2.6 Creating the region R	14
2.7 Showing E_M is C^2 on $h_{18}^{-1}(R)$	15
2.8 Finding a Critical Knot Conformation for E_M	20
2.9 Future Work	24
3 COMPLEMENTARY DOMAINS OF ARRANGEMENTS	25
3.1 Origin of the Problem	25
3.2 Intersection Lattices and Homology	27
3.3 Bezout's Theorem	30
3.4 General Position	30
3.5 Complementary Domains of Algebraic Curves.	31
3.6 Complementary Domains of Ellipsoids	36
3.7 Future Work	39
4 INSCRIBED POLYGONS UNDER ARCLENGTH PRESERVING ISOTOPIES	40
4.1 Definitions	40
4.2 Creating the Polygon	41
4.3 Arclength Preserving Isotopies	46
4.4 Future Work	47
APPENDIX	
A ENERGY MINIMIZATION EXPERIMENT	48
A.1 Gradient Descent Algorithm	48

A.2	Basic Functions	52
A.3	Arclength	53
A.4	Minimum Distance Function	54
B	FINDING THE ENERGY ON THE BOUNDARY OF R	58
B.1	Maple Experiment	58
	REFERENCES	65

LIST OF FIGURES

Figure

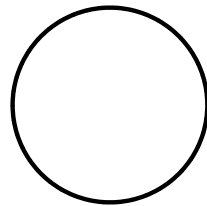
1.1	Same knot type, different energy	1
2.1	A dihedral knot. (Maple)	7
3.1	Complex for ellipsoid example.	29
3.2	Complex for ellipse example	31
3.3	The subcomplex $\Delta(\mathcal{P}_{<\hat{i}})$ for ellipse example.	32
3.4	The hexagon D_a	38

CHAPTER 1 INTRODUCTION

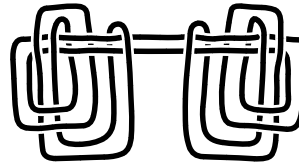
My research concentrates on two subjects within geometric topology: knot energies and complementary domains of arrangements.

1.1 Outline of Chapter 2

In chapter 2, we find a critical knot of the minimum distance knot energy, E_M , which is an energy defined on piecewise linear knots. A knot energy is a functional on knot conformations, or embeddings of a circle into \mathbb{R}^3 , which yields information about qualities of the conformation such as electrical charge, thickness, or tangledness. For instance, both of the conformations below have the same knot type. Their energies, using E_M or others, are very different.



(a) low energy.
(KnotPlot)



(b) higher energy.
(KnotPlot)

Figure 1.1: Same knot type, different energy

I use Processing, a Java-based programming language, to run gradient descent experiments on six segment polygonal trefoil knots. In these experiments, the resulting knot always seems to have dihedral symmetry. We conjecture that the minimum knot for E_M is indeed dihedral. This chapter proves that there exists a dihedral symmetric knot that is a critical point for E_M and is very close to the computer's estimated minimum.

We first numerically find an estimated critical knot K_0 in the space of dihedral knots. We make a small neighborhood R around it and show that the knots on the boundary of R have higher energy K_0 . We then begin a gradient descent from K_0 . The higher energy around the edge prevents the descent trajectory γ from leaving R . The structure imposed on the trajectory by the gradient field promises that a fixed point K^* of E_M is contained in the ω -limit set of γ , which is contained in R . Thus K^* is our desired critical point.

Future projects will aim towards proving that K^* is actually a minimum.

1.2 Outline of Chapter 3

When embedding a collection of codimension 1 algebraic hypersurfaces in a space, the surfaces may separate the space into a number of path components called complementary domains. Finding the number of complementary domain can be difficult even when the intersections between the surfaces are known. We find an *a priori* upper bound for complementary domains for many types of codimension 1 hypersurfaces in \mathbb{R}^2 and \mathbb{R}^3 .

We use a theorem of Ziegler and Živaljević to calculate the number of complementary domains in various situations. We start with a particular arrangement of hypersurfaces \mathcal{A} . We first create a poset \mathcal{P} of all of the hypersurfaces and their intersections. This set is partial ordered by reverse inclusion. We construct $\Delta(\mathcal{P})$, a complex created from \mathcal{P} . The homology of $\Delta(\mathcal{P})$ is closely related to that of the arrangement \mathcal{A} . This is unhelpful if one doesn't quite know how the hypersurfaces in question intersect. This machine would give an exact solution if we specify all the multiple intersections but even without this exact data, we can find upper bounds.

We can provide ourselves with an upper bound for the number of complementary domains of hypersurfaces, even if their intersection is unknown. Utilizing Bezout's Theorem and some basic geometry, we can make statements about the

structure of complex $\Delta(\mathcal{P})$. This will lead us to upper bounds on the complementary domains.

1.3 Outline of Chapter 4

Chapter 4 displays the beginnings of a project relating to thick isotopies. Thick isotopies are defined as isotopies of smooth simple closed curves in \mathbb{R}^3 that preserve the ropelengths of the curves. Eventually, we intend to prove that there are knot conformations K_1 and K_2 which, despite being the same knot type, does not have a thick isotopy from one to the other. Our first step on the way to this result is forming a connection between the ropelength of a smooth curve and polygon inscribed inside it. We expect to use polygons like these help us run computational experiments on these thick knots.

CHAPTER 2

MINIMUM DISTANCE ENERGY FUNCTION MINIMIZERS

Traditionally, an energy function on knots (smooth or polygonal) in \mathbb{R}^3 has been given the following definition.

A function $E : \mathcal{K} \rightarrow \mathbb{R}$ on a collection of conformations \mathcal{K} is called an *energy function* on that collection if:

1. $E(K) \geq 0$ for all $K \in \mathcal{K}$
2. E is invariant under translations, rotations, and scaling of the conformation.
3. As the knot K approaches self intersection, $E(K) \rightarrow \infty$.

Knot energies have been utilized in both biology and particle physics. In biology, different classes of enzymes arrange circular DNA into a variety of knot types. Knot energies and gel electrophoresis provide a more efficient way of identifying the created knot types [2]. In physics, charged knotted tubes (magnetic flux tubes) are used to model glueballs, certain subatomic particles. The glueball spectra of various knot types are predicted using the energy of their minimal conformations [1].

The first knot energy was introduced by Fukuhara [4] in 1988. Shortly afterward, O'Hara [8] defined Möbius energy, which was inspired by the forces exerted on a conformation when an electrical charge is introduced. Minimum distance energy was first introduced by Simon [12] as the piecewise linear analogue to Möbius energy. We will find a critical knot for the minimum distance energy function.

2.1 Basic Definitions

Definition 2.1. *If x, y are points in \mathbb{R}^3 , define $d(x, y)$ to be the distance between x and y under the standard Euclidean metric. If S is a subset of \mathbb{R}^3 , let $d(x, S) = \inf\{d(x, y) | y \in S\}$. If R is another subset of \mathbb{R}^3 , let $d(R, S) = \inf\{d(x, y) | x \in R, y \in S\}$.*

$R, y \in S\}$.

Definition 2.2. We define a **knot conformation** to be an embedding of S^1 into \mathbb{R}^3 .

Definition 2.3. A **polygonal** knot conformation is an embedding which is also a polygon.

Definition 2.4. A piecewise smooth curve in \mathbb{R}^3 is **simple** if it does not intersect itself.

For the purposes of this paper, we will only be considering simple closed six segment polygonal knot conformations. We will often refer to a knot conformation, more simply, as a knot. This is not to be confused with referring to knot type as a knot, as is convention in some other papers.

Definition 2.5. A knot is called **symmetric** if there exist nontrivial rotations of \mathbb{R}^3 under which the vertices of the knot are permuted cyclically. Note that for any given knot, these rotations form a group.

Definition 2.6. A knot is called **dihedral** if a subset of its group of rotations is isomorphic to a dihedral group.

2.2 Understanding Six Segment Dihedral Knots

In this paper, when we call a knot dihedral, we will assume that its symmetry group is \mathbf{D}_3 . Let's spend a moment describing the shape that dihedral knots take. Let $K \subset \mathbb{R}^3$ be a six segment dihedral polygonal knot.

The group \mathbf{D}_3 acts on K via rotations of \mathbb{R}^3 . Take an element of order 3 from \mathbf{D}_3 and call it ρ . Take an order two element and call it σ . These two elements generate \mathbf{D}_3 . Any any element of \mathbf{D}_3 will take vertices of K to vertices of K . Thus ρ is essentially a permutation of the vertices of K of order three. Let $v_1 \in \mathbb{R}^3$ be a vertex of K with order 3 under ρ . Denote $\rho \cdot v_1 = v_3$ and $\rho \cdot v_3 = v_5$. Also denote $\sigma \cdot v_1 = v_2$, $\sigma \cdot v_3 = v_6$, and $\sigma \cdot v_5 = v_4$. If \mathbf{D}_3 is to act nontrivially on K , then none

of the v_i can be fixed under ρ or σ .

Let A denote the set of points that is the axis of rotation of ρ . The vertices v_1, v_3 , and v_5 are all the same distance from A . Likewise, the vertices v_2, v_4 , and v_6 are the same distance from A . Since the order of ρ is 3, the angle of rotation around A is $2\pi/3$. Call the plane containing v_1, v_3 , and v_5 by \mathbf{P}_+ , and the plane containing vertices v_2, v_4 , and v_6 by \mathbf{P}_- . Note that \mathbf{P}_+ and \mathbf{P}_- are parallel planes. Let $c_+ = \mathbf{P}_+ \cap A$ and $c_- = \mathbf{P}_- \cap A$. Since $c_+ = (v_1 + v_3 + v_5)/3$, we have $\sigma(c_+) = \sigma((v_1 + v_3 + v_5)/3) = (\sigma(v_1) + \sigma(v_3) + \sigma(v_5))/3 = (v_2 + v_4 + v_6)/3 = c_-$. As rotations are distance-preserving, we find that all of the vertices are the same distance from A .

We will now decide where the segments are in K . Let S_1 be a segment of K . If the endpoints of S_1 were to lie on the same circle, then by symmetry, K would have two separate components. This means the any segment of K must have endpoints in both \mathbf{P}_+ and \mathbf{P}_- . Without loss of generality, let v_1 and v_2 be the endpoints of S_1 . We see that ρ rotates S_1 through three other segments of K : S_3 (from v_3 to v_4) and S_5 (from v_5 to v_6). Now consider S_2 (having one endpoint at v_2). By the above argument, the other endpoint of S_2 is either v_3 or v_5 . Afterwards the rest of the segments of K follow through symmetry. Note that if S_2 ends in v_3 then all vertices are in cyclic order as we travel around the knot. If S_2 ends in v_5 , we may simply reindex to achieve this cyclic ordering.

Thus for any six segment \mathbf{D}_3 -knot K , the vertices of K lie in a pair of coaxial circles of the same radius. Each circle contains three vertices, and these vertices divide the circle evenly into thirds. Each segment of the knot has as its endpoints one vertex from each circle. Further, the knot travels around each circle in the same direction.

We wish to define values r and θ , which will identify a particular conformation of dihedral knot, up to scaling and rigid motion. Let K be a dihedral knot. Without

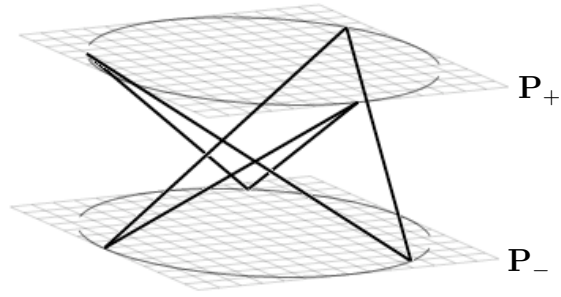


Figure 2.1: A dihedral knot. (Maple)

loss of generality, let the axis of K be the z -axis. Let the indexing of the vertices (within the planes) increase in the clockwise direction as you view the knot from the positive z direction. Let r be the ratio between the distance between the planes \mathbf{P}_+ and \mathbf{P}_- versus the radii of the coaxial circles that contain the points. Let θ be the angle from the vector $v_1 - c_+$ to the vector $v_2 - c_-$. There are two cases:

- *Case 1: \mathbf{P}_- has a smaller z -value than \mathbf{P}_+ .* If θ is in the interval $(-\pi_3, \pi)$, (or a coterminal interval of angles) then K is unknotted. If $\theta \in (\pi, 4\pi/3)$, then K is a right-handed trefoil. If $\tilde{\theta} \in (4\pi/3, 5\pi/3)$, then K is a left-handed trefoil. The knot K is self intersecting at any other value of θ .
- *Case 2: \mathbf{P}_- has a larger z -value than \mathbf{P}_+ .* If θ is in the interval $(-\pi_3, \pi)$, then K is unknotted. If $\theta \in (\pi, 4\pi/3)$, then K is a left-handed trefoil. If $\theta \in (4\pi/3, 5\pi/3)$, then K is a right-handed trefoil. The knot K is self intersecting at any other value of θ .

In Case 1, segment S_1 is longer than segment S_2 . In Case 2, segment S_2 is longer than segment S_1 . However, the knots in the two cases are the same (after a shifting of indices). A knot from Case 1 with $r = \hat{r}$ and $\theta = \hat{\theta}$ can be changed into the Case 2 knot with $r = \hat{r}$ and $\theta = 8\pi/3 - \hat{\theta}$ with a rotation.

We can now refer to any left-handed dihedral knot, up to scaling and rigid

motion, by an ordered pair (r, θ) . We lose no generality in assuming that $4\pi/3 \leq \theta \leq 5\pi/3$ so that we remain in Case 1.

2.3 Definitions

We will be working over two spaces: \mathbb{R}^{18} and \mathbb{R}^2 . We will need to create a version of the minimum distance energy function for both of them. We will first create the energy function in \mathbb{R}^{18} and then use a map to extend it to \mathbb{R}^2 .

Definition 2.7. Let the projection $v_k : \mathbb{R}^{18} \longrightarrow \mathbb{R}^3$ be defined as

$$v_k(\mathbf{x}) = (x_{3k-2}, x_{3k-1}, x_{3k})$$

for $k = 1, \dots, 6$.

Definition 2.8. Let the function $w_k : \mathbb{R}^{18} \longrightarrow \mathbb{R}^3$ be defined by $w_k(\mathbf{x}) = v_{k+1}(\mathbf{x}) - v_k(\mathbf{x})$ for $k = 1, \dots, 5$ and let $w_6(\mathbf{x}) = v_1(\mathbf{x}) - v_6(\mathbf{x})$.

We may identify each point \mathbb{R}^{18} with a six segment polygon in \mathbb{R}^3 . The point $\mathbf{x} \in \mathbb{R}^{18}$ is identified with the polygon $\{(v_1(\mathbf{x}), v_2(\mathbf{x}), v_3(\mathbf{x}), v_4(\mathbf{x}), v_5(\mathbf{x}), v_6(\mathbf{x}))\}$ (If we allow for repeated points and self intersection.)

We will restrict ourselves to a subset of \mathbb{R}^{18} that more closely matches our concept of what a polygon should look like.

Definition 2.9. Define $\mathcal{K} \subset \mathbb{R}^{18}$ to be the collection of all $\mathbf{x} \in \mathbb{R}^{18}$ that satisfy:

- $v_i(\mathbf{x}) \neq v_j(\mathbf{x})$ for $i \neq j$.
- $(v_{i+2}(\mathbf{x}) - v_{i+1}(\mathbf{x})) \times (v_{i+1}(\mathbf{x}) - v_i(\mathbf{x})) \neq \mathbf{0}$

for all $i = 1, \dots, 6$.

Definition 2.10. Define $c : \mathcal{K} \longrightarrow \mathbb{R}^3$ by $c(\mathbf{x}) = (c_1(\mathbf{x}), c_2(\mathbf{x}), c_3(\mathbf{x})) = \frac{1}{6}(v_1(\mathbf{x}) + \dots + v_6(\mathbf{x}))$.

Definition 2.11. Define $\hat{c} : \mathcal{K} \longrightarrow \mathbb{R}^{18}$ by $\hat{c}(\mathbf{x}) = (c_1(\mathbf{x}), c_2(\mathbf{x}), c_3(\mathbf{x}), c_1(\mathbf{x}), \dots, c_3(\mathbf{x}))$.

Definition 2.12. Let $\tilde{\mathcal{K}} = \{\mathbf{x} \in \mathcal{K} : v_1(\mathbf{x}) + \dots + v_6(\mathbf{x}) = \mathbf{0}, \|v_2(\mathbf{x}) - v_1(\mathbf{x})\| = 1\}$.

Definition 2.13. Let $g : \mathcal{K} \rightarrow \tilde{\mathcal{K}}$ be defined by

$$g(\mathbf{x}) = \frac{1}{\|v_2(\mathbf{x}) - v_1(\mathbf{x})\|}(\mathbf{x} - \hat{c}(\mathbf{x}))$$

Definition 2.14. Let $\mathbf{x} \in \mathbb{R}^{18}$. Define $S_i : \mathbb{R}^{18} \rightarrow \{\text{Segments in } \mathbb{R}^3\}$ by having $S_i(\mathbf{x})$ be the segment in \mathbb{R}^3 with endpoints $v_i(\mathbf{x})$ and $v_{i+1}(\mathbf{x})$.

Definition 2.15. Let $\mathbf{x} \in \mathbb{R}^{18}$. Define $L_i : \mathbb{R}^{18} \rightarrow \{\text{Lines in } \mathbb{R}^3\}$ by having $L_i(\mathbf{x})$ be the line in \mathbb{R}^3 with through the points $v_i(\mathbf{x})$ and $v_{i+1}(\mathbf{x})$.

Definition 2.16. We call a point $\mathbf{x} \in \mathbb{R}^{18}$ **dihedral** if there exists:

- A group of rotations $A_x = \{A_1, \dots, A_6\}$ so that A_x is isomorphic to D_3 and each A_i is a block matrix with the blocks a rotation of \mathbb{R}^3 .
- A group of permutations $P_x = \{P_1, \dots, P_6\}$ so that $A_i(\mathbf{x}) = P_i(\mathbf{x})$.

A way to find r and θ , given a dihedral knot in \mathbb{R}^{18} was described in the “Understanding Six Segment Dihedral Knots” section. We will define these as functions.

Definition 2.17. Let $D = \{\mathbf{x} \in \mathbb{R}^{18} \mid \mathbf{x} \text{ is dihedral}, \theta(\mathbf{x}) \in (4\pi/3, 5\pi/3), \text{length}(S_1(\mathbf{x})) > \text{length}(S_2(\mathbf{x}))\}$. Let $c_+(\mathbf{x}) = \frac{1}{3}(v_1(\mathbf{x}) + v_3(\mathbf{x}) + v_5(\mathbf{x}))$ and $c_-(\mathbf{x}) = \frac{1}{3}(v_2(\mathbf{x}) + v_4(\mathbf{x}) + v_6(\mathbf{x}))$. Define the map $r : D \rightarrow \mathbb{R}$ by $r(\mathbf{x}) = |c_+(\mathbf{x}) - c_-(\mathbf{x})|$. Define $\theta : D \rightarrow \mathbb{R}$ by $\angle(v_1(\mathbf{x}) - c_+(\mathbf{x}), v_2(\mathbf{x}) - c_-(\mathbf{x}))$ where \angle is the angle from vector $v_1(\mathbf{x}) - c_+(\mathbf{x})$ to vector $v_2(\mathbf{x}) - c_-(\mathbf{x})$ as measured counterclockwise from the $c_+(\mathbf{x}) - c_-(\mathbf{x})$ direction.

Definition 2.18. Define $\tilde{\mathcal{K}} = \{(r, \theta) \in \mathbb{R}^2 : r \in (0, \infty), \theta \in (4\pi/3, 5\pi/3)\}$.

Definition 2.19. Define the map $h_{18} : D \rightarrow \mathbb{R}^2$ by $h_{18}(\mathbf{x}) = (r(\mathbf{x}), \theta(\mathbf{x}))$.

Definition 2.20. Let $h_2 : \tilde{\mathcal{K}} \rightarrow \mathcal{K}$ be defined by $h_2(r, \theta) = (x_1, \dots, x_{18})$ where,

$$\begin{aligned} (x_1, x_2, x_3) &= (1, 0, 2r) \\ (x_4, x_5, x_6) &= (\cos(\theta), \sin(\theta), 0) \\ (x_7, x_8, x_9) &= \left(-\frac{1}{2}, \frac{\sqrt{3}}{2}, 2r\right) \\ (x_{10}, x_{11}, x_{12}) &= \left(\cos\left(\theta + \frac{2\pi}{3}\right), \sin\left(\theta + \frac{2\pi}{3}\right), 0\right) \\ (x_{13}, x_{14}, x_{15}) &= \left(-\frac{1}{2}, -\frac{\sqrt{3}}{2}, 2r\right) \\ (x_{16}, x_{17}, x_{18}) &= \left(\cos\left(\theta + \frac{4\pi}{3}\right), \sin\left(\theta + \frac{4\pi}{3}\right), 0\right) \end{aligned}$$

Definition 2.21. Define $f : \bar{\mathcal{K}} \rightarrow \tilde{\mathcal{K}}$ by $f(r, \theta) = (g \circ h_2)(r, \theta)$.

Definition 2.22. Let K be an n -segment polygonal knot with segments S_1, \dots, S_n . Define the (i, j) minimum distance function $M_{i,j} : \mathbb{R}^{3n} \rightarrow \mathbb{R}$ by $M_{i,j}(\mathbf{x}) = d(S_i(\mathbf{x}), S_j(\mathbf{x}))$.

Definition 2.23. Let S be a line segment in \mathbb{R}^3 . Call the endpoints of S by s_0 and s_1 . Let L be the line containing S . Place an ordering on L so that $s_0 < s_1$. Let $\mathbf{y} \in \mathbb{R}^3 \setminus L$. Define $\pi_S : \mathbb{R}^3 \setminus L \rightarrow S$ by

$$\pi_S(\mathbf{y}) = \begin{cases} c_{\mathbf{y}} & \text{if } s_0 \leq c_{\mathbf{y}} \leq s_1 \\ s_0 & \text{if } c_{\mathbf{y}} < s_0 \\ s_1 & \text{if } s_1 < c_{\mathbf{y}} \end{cases}$$

where $c_{\mathbf{y}} = \text{proj}_L(\mathbf{y})$ is the closest point of L to \mathbf{y} .

2.4 The Minimum Distance Energy Function

In this section, we will define the minimum distance energy functions and discuss their smoothness.

Lemma 2.24. The function π_S is continuously differentiable on \mathbb{R}^3 except on a set of measure zero.

Proof. First, π_S is a constant function on the sets $\{x \in \mathbb{R}^3 | c_x < s_0\}$ and $\{x \in \mathbb{R}^3 | s_1 < c_x\}$. Further, in $\{x \in \mathbb{R}^3 | s_0 < c_x < s_1\}$, $\pi_S(x)$ is just projection of x onto L , which is continuously differentiable. Finally the set $\{x \in \mathbb{R}^3 | c_x = s_0 \text{ or } c_x = s_1\}$ is just a pair of parallel planes and thus is of measure zero. \square

Lemma 2.25. Let S be a line segment in \mathbb{R}^3 . Let \mathbf{y} be a point not on the line L identified by S . Then $d(\mathbf{y}, S) = d(\mathbf{y}, \pi_S(\mathbf{y}))$.

Proof. Note that the vector $c_{\mathbf{y}} - \mathbf{y}$ is orthogonal to L . Let $\mathbf{s} \in S$. Since $d(c_{\mathbf{y}}, \pi_S(\mathbf{y})) < d(c_{\mathbf{y}}, \mathbf{s})$, we have $d(\mathbf{y}, \pi_S(\mathbf{y})) < d(\mathbf{y}, \mathbf{s})$. \square

Any two disjoint non-parallel lines L_i and L_j in \mathbb{R}^3 have a pair of closest points d_i and d_j . The segment joining d_i and d_j is orthogonal to both L_i and L_j . We will call d_i and d_j the double critical pair on L_i and L_j .

Lemma 2.26. *Let \mathbf{x} be a knot in \mathbb{R}^{18} . Parametrize lines $L_i(\mathbf{x})$ and $L_j(\mathbf{x})$ by $\alpha_i(t) = (1-t)v_i(\mathbf{x}) + tv_{i+1}(\mathbf{x})$ and $\alpha_j(t) = (1-t)v_j(\mathbf{x}) + tv_{j+1}(\mathbf{x})$. Let the double critical pair of points on L_i and L_j be $\alpha(d_i)$ and $\alpha(d_j)$. Let $\pi_i = \pi_{L_i}$. Then*

$$M_{i,j}(\mathbf{x}) = \begin{cases} d(L_i(\mathbf{x}), L_j(\mathbf{x})) & \text{if } 0 < d_i < 1 \text{ and } 0 < d_j < 1 \\ m_{i,j}(\mathbf{x}) & \text{if otherwise} \end{cases},$$

where $m_{i,j}(\mathbf{x}) = \min\{d(v_i, \pi_j(v_i)), d(v_{i+1}, \pi_j(v_{i+1})), d(\pi_i(v_j), v_j), d(\pi_i(v_{j+1}), v_{j+1})\}$

Proof. Let $s_i \in S_i(\mathbf{x})$ and $s_j \in S_j(\mathbf{x})$. Let S be the segment joining s_i and s_j . Let D be the segment joining $\alpha(d_i)$ and $\alpha(d_j)$. Consider a linear homotopy moving S into D . Under this homotopy, s_i is moved along the line L_i towards $\alpha(d_i)$. Likewise s_j moves along L_j towards $\alpha(d_j)$. There are a couple of cases:

- *Case 1:* ($\alpha(d_i) \in S_i$, $\alpha(d_j) \in S_j$) In this case, $d(\alpha(d_i), \alpha(d_j)) = d(L_i, L_j) \leq d(s_i, s_j)$.
- *Case 2:* (*Otherwise*) We can write the length of S in term of its component in the direction of D and orthogonal to the direction of D : $length(S) = \sqrt{length_D(S)^2 + length_{\perp}(S)^2}$ As we homotope S toward D , the value of $length_D(S)$ does not change. However, $length_{\perp}(S)$ will decrease as we move S to D . We are going to stop this homotopy the first time one of the endpoints of S coincides with v_i, v_{i+1}, v_j , or v_{j+1} . From there, we can use the previous lemma to find the closest point in the opposing line. For instance, say we end up with a line segment that has v_i as one of its endpoints. The other endpoint is still in S_j . The closest point in S_j to v_i is $\pi_j(v_i)$. Thus $d(v_i, \pi_j(v_i)) \leq d(s_i, s_j)$. This can be done for any of the endpoints v_i, v_{i+1}, v_j , or v_{j+1} .

□

Lemma 2.27. *The function $M_{i,j}$ is continuously differentiable except on a set of measure zero.*

Proof. The function $M_{i,j}$ is defined in a piecewise manner. Both $d(L_i(\mathbf{x}), L_j(\mathbf{x}))$ and $m_{i,j}(\mathbf{x})$ are continuously differentiable except on a set of measure zero. We must show that the boundaries of the regions over which the function is defined form a set of measure zero. The boundaries occur where d_i equals 0 or 1 and where d_j equals 0 or 1. They also exist whenever the minimum function changes. The set of points \mathbf{x} where $d_i(\mathbf{x})$ equals 0 or 1 lies on a pair of planes, and thus has measure zero.

Let $M_{i,j}(K) = m_0$.

Case 1: $d(v_i, \pi_j(v_i)) = m_0$

Consider the set $C = \{p \in \mathbb{R}^3 | d(p, \pi_i(p)) = m_0\}$. Let the open cylindrical portion of the set C be called B . Let the two hemispheres be called A_{v_i} and $A_{v_{i+1}}$ respectively. Firstly, $\pi_j(v_i)$ lies on A_{v_i} . If there is another point of S_j intersecting C , then either there is a point of S_j closer to S_i than $\pi_j(v_i)$ (which is impossible), or S_j and S_i are parallel. The set of knots with parallel S_j and S_i is measure zero.

Subcase 1a: Let $\pi_j(v_i)$ be an endpoint of S_j . Then our knot is in the set $\{K \in \mathbb{R}^{3n} | d(v_i, v_j) = m_0 \text{ or } d(v_i, v_{j+1}) = m_0\}$, which is a set of measure zero.

Subcase 1b: Let $\pi_j(v_i)$ be an interior point of S_j . Then our knot is in the set $\{K \in \mathbb{R}^{3n} | d(v_i, L_j) = m_0\}$ is a set of measure zero.

Cases 2 - 4: Similar to case 1. □

Definition 2.28. *Let $\mathcal{S}_K = \{(S_i, S_j) : S_i, S_j \text{ are non-adjacent segments of } K, i \leq j\}$*

We will now create the minimum distance energy function.

Definition 2.29. *Define the minimum distance energy function on \mathcal{K} , $E_M :$*

$\mathcal{K} \longrightarrow \mathbb{R}$ by

$$E_M(\mathbf{x}) = \sum_{(S_i, S_j) \in \mathcal{S}_{\mathcal{K}}} \frac{\|v_{i+1}(\mathbf{x}) - v_i(\mathbf{x})\| \cdot \|v_{j+1}(\mathbf{x}) - v_j(\mathbf{x})\|}{d(S_i(\mathbf{x}), S_j(\mathbf{x}))^2}.$$

Definition 2.30. Let $\tilde{E} = E|_{\tilde{\mathcal{K}}}$.

Note also that $E(\mathbf{x}) = \tilde{E}(g(\mathbf{x}))$.

We also wish to define an energy function on \mathbb{R}^2 so that we may apply it to our chosen form of dihedral knots.

Definition 2.31. Define the **minimum distance energy function on $\bar{\mathcal{K}}$** $\bar{E}_M : \bar{\mathcal{K}} \longrightarrow \mathbb{R}$ by $\bar{E}_M(r, \theta) = (E_M \circ h_2)(r, \theta)$.

Note also that $E(\mathbf{x}) = \bar{E}(h_{18}(\mathbf{x}))$ for all dihedral knots $\mathbf{x} \in D$.

Proposition 2.32. The function E_M is continuously differentiable except on a set of measure zero.

Proof. The function E_M is continuously differentiable exactly where all of its $M_{i,j}$ functions are continuously differentiable. Since each of these $M_{i,j}$ fail to be continuously differentiable only on a set of measure zero, the function E_M fails to be C^1 only on the union of these sets. \square

With all of our energy functions defined we are going to create a more continuous function on the spaces \mathbb{R}^{18} and \mathbb{R}^2 . This function will be equal to the energy function, provided that the distance between all segments of the knot is simply the distance between the lines containing the segments.

Definition 2.33. We define $E_C : \mathbb{R}^{18} \longrightarrow \mathbb{R}$ to be

$$E_C(\mathbf{x}) = \sum_{(S_i, S_j) \in \mathcal{S}_{\mathcal{K}}} \frac{\text{length}(S_i(\mathbf{x})) \cdot \text{length}(S_j(\mathbf{x}))}{d(L_i(\mathbf{x}), L_j(\mathbf{x}))^2}$$

Note that E_C is C^2 wherever it is defined.

Definition 2.34. We define $\bar{E}_C : \mathbb{R}^2 \longrightarrow \mathbb{R}$ by $\bar{E} = E \circ h_2$.

2.5 Preview of Coming Attractions

The next steps in the proof can be a bit complicated, so we will provide a quick summary of the remainder of Chapter 2 before we continue. We suspect that the minimum knot conformation K^* for E_M in \mathbb{R}^{18} is dihedral. It may be easier, computationally, if we find a critical knot for \bar{E}_M instead. The function \bar{E}_C is the same as \bar{E}_M for many values in \mathbb{R}^2 . Further, \bar{E}_C is C^2 where $d(L_i, L_j)$ is nonzero. We find an estimated critical knot conformation for \bar{E}_C , using Maple to calculate it. Using this, we create a very small region R that contains a minimum of \bar{E}_C . We will show that $E_C = E_M$ on the interior of $h_{18}^{-1}(R)$ in order to prove that E_M is C^2 on $h_{18}^{-1}(R)$. This will prove that \tilde{E}_M is C^1 on $h_{18}^{-1}(R) \cap \tilde{\mathcal{K}}$. Finally, we will use gradient descent to find a critical knot in $h_{18}^{-1}(R) \cap \tilde{\mathcal{K}}$. From this, we get a critical conformation in \mathbb{R}^{18} .

2.6 Creating the region R .

There have been a number computational experiments, written in a variety of programming languages, intending to find the lowest energy states of various knot types. Some of these are gradient descent experiments that have been written for polygonal knots using the minimum distance function. I have written one of my own in a programming language called Processing. Processing is an open source programming language and environment. My code for the experiment can be found in Appendices A.1 through A.4.

After writing the code necessary for the descent experiment, I ran the experiment on a number of right handed six segment trefoil knots. The resulting knots always looked very dihedral. Further, the r and θ values for these knots always ended up being approximately .5 and 4.6, respectively. It appeared that a critical knot for the MD-energy might be dihedral.

While we are unable to explicitly solve the system $\nabla \bar{E}_C = 0$, we are able to get a great estimation by solving numerically. We get $\bar{E}_C(0.5261243504, 4.642845642) \simeq$

0. Let $r_0 = 0.5261243504$ and $\theta_0 = 4.642845642$. Define the region $R = \{(r, \theta) \mid |r - r_0| < .01, |\theta - \theta_0| < .01\}$.

2.7 Showing E_M is C^2 on $h_{18}^{-1}(R)$

Next, we shall show that E_M is C^2 on $h_{18}^{-1}(R)$. We will do this by showing that $E_M = E_C$ on $h_{18}^{-1}(R)$. Let $y = h_2(r, \theta)$ and $y_0 = h_2(r_0, \theta_0)$.

Lemma 2.35. *For y_0 as defined above, $|v_i(\mathbf{y}_0) - v_j(\mathbf{y}_0)| \leq \sqrt{4 + 4r_0^2}$.*

Proof. We use the Pythagorean Theorem. The vertices of the knot are contained in the cylinder $x^2 + y^2 = 1$ embedded in \mathbb{R}^3 . No two points in y_0 are farther from each other than the points $(1, 0, 2r_0)$ and $(-1, 0, 0)$. \square

Lemma 2.36. *Let $\rho > 0$. Let $|r(\mathbf{y}) - r_0| < \rho$ and $|\theta(\mathbf{y}) - \theta_0| < \rho$. Then $|v_k(\mathbf{y}) - v_k(\mathbf{y}_0)| < 3\rho$*

Proof. Then

$$\begin{aligned} |v_i(\mathbf{y}) - v_i(\mathbf{y}_0)| &\leq |(\cos(\theta - \alpha), \sin(\theta - \alpha), 2r) - (\cos(\theta_0 - \alpha), \sin(\theta_0 - \alpha), 2r_0)| \\ &= (\cos(\theta - \alpha) - \cos(\theta_0 - \alpha))^2 + (\sin(\theta - \alpha) - \sin(\theta_0 - \alpha))^2 \\ &\quad + (2(r - r_0))^2 \\ &\leq |\theta - \theta_0| + 2|r - r_0| \\ &= 3\rho \end{aligned}$$

where α is 0, $2\pi/3$, or $4\pi/3$ \square

Lemma 2.37. *Let $\rho > 0$. Let $|r(\mathbf{y}) - r_0| < \rho$ and $|\theta(\mathbf{y}) - \theta_0| < \rho$. Then $|(v_i(\mathbf{y}) - v_j(\mathbf{y})) \cdot (v_k(\mathbf{y}) - v_l(\mathbf{y})) - (v_i(\mathbf{y}_0) - v_j(\mathbf{y}_0)) \cdot (v_k(\mathbf{y}_0) - v_l(\mathbf{y}_0))| < 24\rho\sqrt{1 + r_0^2} + 36\rho^2$*

Proof. Let $a = (v_i(\mathbf{y}) - v_j(\mathbf{y})) - (v_i(\mathbf{y}_0) - v_j(\mathbf{y}_0))$ and $b = (v_k(\mathbf{y}) - v_l(\mathbf{y})) - (v_k(\mathbf{y}_0) - v_l(\mathbf{y}_0))$

$v_l(\mathbf{y}_0)$). Then $|a|, |b| < 6\rho$ by Lemma 2.36. Then

$$\begin{aligned}
& |(v_i(\mathbf{y}) - v_j(\mathbf{y})) \cdot ((v_k(\mathbf{y}) - v_l(\mathbf{y}))) \\
& - (v_i(\mathbf{y}_0) - v_j(\mathbf{y}_0)) \cdot (v_k(\mathbf{y}_0) - v_l(\mathbf{y}_0))| \\
& = |(v_i(\mathbf{y}_0) - v_j(\mathbf{y}_0) + a) \cdot (v_k(\mathbf{y}_0) - v_l(\mathbf{y}_0) + b) \\
& - (v_i(\mathbf{y}_0) - v_j(\mathbf{y}_0)) \cdot (v_k(\mathbf{y}_0) - v_l(\mathbf{y}_0))| \\
& = |a \cdot (v_k(\mathbf{y}_0) - v_l(\mathbf{y}_0)) + b \cdot (v_i(\mathbf{y}_0) - v_j(\mathbf{y}_0)) + a \cdot b| \\
& \leq 6\rho|v_k(\mathbf{y}_0) - v_l(r_0, \theta_0)| + 6\rho|(v_i(\mathbf{y}_0) - v_j(\mathbf{y}_0))| + 36\rho^2 \\
& \leq 12\rho\sqrt{4 + 4r_0^2} + 36\rho^2 = 24\rho\sqrt{1 + r_0^2} + 36\rho^2
\end{aligned}$$

by Lemma 2.47 □

Definition 2.38. *Define*

$$T(x, i, j, q) = \frac{(w_i \cdot w_j + q)(w_j \cdot (v_i - v_j) + q) - (w_j \cdot w_j - q)(w_i \cdot (v_i - v_j) - q)}{(w_i \cdot w_i - q)(w_j \cdot w_j - q) - (w_i \cdot w_j + q)^2},$$

where $w_i = w_i(\mathbf{x}), w_j = w_j(\mathbf{x})$ are defined as above and q is a real number defined as above.

Theorem 2.39. *For all $\mathbf{x} \in h_{18}^{-1}(R)$, $E_C(\mathbf{x}) = E_M(\mathbf{x})$ holds.*

Proof. Consider a knot $\mathbf{x} \in h_{18}^{-1}(R)$. By symmetry, we can see that the segments $S_i(\mathbf{x})$ can be one of two lengths, and the the segment lengths alternate as we continue around the knot. The segments $S_1(\mathbf{x}), S_3(\mathbf{x}),$ and $S_5(\mathbf{x})$, which are all of the same length, will be called 1-segments. Likewise the segments $S_2(\mathbf{x}), S_4(\mathbf{x}),$ and $S_6(\mathbf{x})$, all of the same length, will be called 2-segments. Because of symmetry, the distance between any two 1-segments is the same. This is true for the distance between 2-segments and the distance between 1-segments and 2-segments. We wish to show that the closest points between a pair of segments of \mathbf{x} is on the interior of the segments. It suffices to do this for one pair of 1- segments, a pair of 2-segments,

and a pair containing one 1-segment and one 2-segment.

Define $\mathbf{y} = h_2(h_{18}(x))$. The knot \mathbf{x} differs from \mathbf{y} only by rigid motion and scaling. Thus, if show that the closest points between a pair of segments of \mathbf{y} is on the interior of the segments, the same will be true of \mathbf{x} .

Let $d_{i,j}$ be the closest point on line $L_j(\mathbf{y})$ to line $L_i(\mathbf{y})$. We wish to show that $v_1(\mathbf{y}) < d_{2,1} < v_2(\mathbf{y})$ and $v_2(\mathbf{y}) < d_{1,2} < v_3(\mathbf{y})$. We begin by parametrizing the lines containing the segments $S_1(\mathbf{y})$ and $S_2(\mathbf{y})$. Let $L_i(t) = v_i + t(v_{i+1} - v_i)$. Let $d_{i,j} = L_j(t_{i,j})$. Then we just wish to show that $0 \leq t_{2,1}, t_{3,1}, t_{4,2} \leq 1$.

We can find $t_{i,j}$ by finding the (s, t) that minimizes the function $f(s, t) = |L_i(s) - L_j(t)|$. The value $t_{j,i}$ will be the value of s that minimizes f . The value of $t_{i,j}$ will follow through symmetry. Some calculation shows that $t_{j,i} = \frac{(w_i \cdot w_j)(w_j \cdot (v_i - v_j)) - (w_j \cdot w_j)(w_i \cdot (v_i - v_j))}{(w_i \cdot w_i)(w_j \cdot w_j) - (w_i \cdot w_j)^2}$, where $w_i = w_i(\mathbf{y})$.

Let $y_0 = h_2(r_0, \theta_0)$. Let $\rho = .01$. By Lemma 2.37, $|(v_i(\mathbf{y}) - v_j(\mathbf{y})) \cdot ((v_k(\mathbf{y}) - v_l(\mathbf{y})) - (v_i(\mathbf{y}_0) - v_j(\mathbf{y}_0))) \cdot (v_k(\mathbf{y}_0) - v_l(\mathbf{y}_0))| < 24\rho\sqrt{1 + r_0^2} + 36\rho^2 \approx 0.274790$. Denote $q_0 = 0.274790$. Written another way,

$$\begin{aligned} (v_i(\mathbf{y}_0) - v_j(\mathbf{y}_0)) \cdot (v_k(\mathbf{y}_0) - v_l(\mathbf{y}_0)) - q_0 &\leq (v_i(\mathbf{y}) - v_j(\mathbf{y})) \cdot (v_k(\mathbf{y}) - v_l(\mathbf{y})) \\ &\leq (v_i(\mathbf{y}_0) - v_j(\mathbf{y}_0)) \cdot (v_k(\mathbf{y}_0) - v_l(\mathbf{y}_0)) + q_0. \end{aligned}$$

Then $T(\mathbf{y}_0, i, j, -q_0) \leq T(\mathbf{y}, i, j, 0) \leq T(\mathbf{y}_0, i, j, q_0)$. Recall that $t_{j,i} = T(\mathbf{y}, i, j, 0)$ by definition.

We compute (in Maple) the values of $T(\mathbf{y}_0, i, j, -q_0)$ and $T(\mathbf{y}_0, i, j, q_0)$ for all i and j required. We find that for any i and j the following inequality holds:

$$\begin{aligned} 0 \leq .09068 &\approx \min_{i,j}(T(K(r_0, \theta_0), i, j, -.18239)) \leq T(K(r, \theta), i, j, 0) = t_{j,i} \\ &\leq \max_{i,j}(T(K(r_0, \theta_0), i, j, .18239)) \approx .87413 \leq 1 \end{aligned}$$

Thus the closest points on any pair of segments $S_i(\mathbf{y})$ and $S_j(\mathbf{y})$ occur in the interior of the segments. As \mathbf{x} differs from \mathbf{y} only by rigid motions and scaling, the same must be true of \mathbf{x} . Since E_M and E_C are identical when $d(S_i, S_j) = d(L_i, L_j)$, $E_M = E_C$ over all of $h_{18}^{-1}(R)$. \square

Proposition 2.40. *There is an open set U containing R so that the function E_M is C^2 on $h_{18}^{-1}(U)$.*

Proof. Consider the knot \mathbf{x} in $h_{18}^{-1}(R)$. We have already shown that if we take a look at the closest points in any two lines $L_i(\mathbf{x})$ and $L_j(\mathbf{x})$ containing segments $S_i(\mathbf{x})$ and $S_j(\mathbf{x})$ in the knot \mathbf{x} we will find that the closest points will be on the interior of S_i and S_j . As $T(\mathbf{x}, i, j, 0)$ changes continuously with \mathbf{x} , there is a neighborhood $N_{\mathbf{x}}$ around \mathbf{x} in \mathbb{R}^{18} of values for which $E_M = E_C$. Let $U = \bigcup_{\mathbf{x} \in h_{18}^{-1}(R)} N_{\mathbf{x}}$. Since all of the closest points are on the interior of the segments, the function E_C will be only be undefined where the knot is self intersecting. The knot is not self intersecting anywhere in $h_{18}^{-1}(U)$, and E_C is C^2 wherever it is defined, so E_M is C^2 on $h_{18}^{-1}(U)$. \square

Next we show that \bar{E}_M has a local minimum in the region R . We will do this by showing that a point in the interior of R has a lower energy than any point on the boundary. By Theorem 2.39, we may use E_C in place of E_M . This will make the calculations faster and easier for Maple to complete. We ask Maple to calculate E_C for a large number of knots on the boundary of R . Evenly spaced around the boundary are 115996 data points making a total of 29000 data points on each side of the rectangle. (The corners are counted twice.) The symmetry of these knots is such that of the nine terms present in E_C there are only three distinct values that a term can take. Each value occurs three times among the terms. We ask Maple to find each of these values on each of the 115996 boundary knots. Finally we add them together to obtain E_C for each boundary knot. We then ask Maple to find the minimum such value; which ends up being 189.9216712. The code corresponding to this experiment can be found in Appendix A.5.

We must show that if we take the minimum over the entire boundary, we will still be close to this value. We are going to let (r_1, θ_1) be one of the 115996 boundary knots that we chose. We will then show that any knot that is close to this one has a similar energy value.

Lemma 2.41. *Let $\rho > 0$. Let r and θ have the property that $|r - r_1| \leq \rho$ and $|\theta - \theta_1| \leq \rho$. Then $|M_{i,j}((r, \theta)) - M_{i,j}((r_1, \theta_1))| \leq 4\rho$*

Proof. The endpoints change by at most 2ρ . Then the segment lies in a 2ρ neighborhood of its original position. Then the distance can't change more than 4ρ . \square

Proposition 2.42. *Let $\rho > 0$. Let r and θ have the property that $|r - r_1| \leq \rho$ and $|\theta - \theta_1| \leq \rho$. Then*

$$|\bar{E}_M(r, \theta) - \bar{E}_M(r_1, \theta_1)| \leq \sum \frac{8l_i l_j m_{i,j} \rho + 16l_i l_j \rho^2 + 2l_j m_{i,j}^2 \rho + 2l_i m_{i,j}^2 \rho - 4\rho^2 m_{i,j}^2}{m_{i,j}^2 (m_{i,j}^2 + 4\rho)^2}$$

where we are summing over non adjacent segments and l_i, l_j are the lengths of the segments of $h_2(r_1, \theta_1)$ and $m_{i,j}$ is the distance between them.

Proof.

$$\begin{aligned} |\bar{E}_M(r, \theta) - \bar{E}_M(r_1, \theta_1)| &\leq \left| \sum \frac{l_i l_j}{m_{i,j}^2} - \sum \frac{(l_i - 2\rho)(l_j - 2\rho)}{(m_{i,j} + 4\rho)^2} \right| \\ &= \sum \left(\frac{l_i l_j}{m_{i,j}^2} - \frac{(l_i - 2\rho)(l_j - 2\rho)}{(m_{i,j} + 4\rho)^2} \right) \\ &= \sum \frac{8l_i l_j m_{i,j} \rho + 16l_i l_j \rho^2 + 2l_j m_{i,j}^2 \rho + 2l_i m_{i,j}^2 \rho - 4\rho^2 m_{i,j}^2}{m_{i,j}^2 (m_{i,j}^2 + 4\rho)^2} \end{aligned}$$

\square

Lemma 2.43. *The function \bar{E}_M has a local minimum in the region R .*

Proof. We have three different terms in the function \bar{E}_M so we will look at the terms individually.

- *The 1,3 term:* We know from Maple that:

1. $l_1 \leq 1.818965707$

2. $l_3 \leq 1.818965707$

3. $.9573654999 \leq m_{1,3} \leq .9827258350$

Then $\left| \frac{l_1 l_3}{m_{1,3}^2} - \frac{(l_1 - 2\rho)(l_3 - 2\rho)}{(m_{1,3} + 4\rho)^2} \right| \leq .00002959264763$ by Proposition 2.42.

- *The 1,4 term:* We know from Maple that:

1. $l_1 \leq 1.818965707$
2. $l_4 \leq 2.195265455$
3. $.3814114756 \leq m_{1,4} \leq .3982874655$

Then $|\frac{l_1 l_4}{m_{1,4}^2} - \frac{(l_1 - 2\rho)(l_4 - 2\rho)}{(m_{1,4} + 4\rho)^2}| \leq .003135336024$ by Proposition 2.42.

- *The 2,4 term:* We know from Maple that:

1. $l_2 \leq 2.195265455$
2. $l_4 \leq 2.195265455$
3. $.3649785397 \leq m_{2,4} \leq .3841949676$

Then $|\frac{l_2 l_4}{m_{2,4}^2} - \frac{(l_2 - 2\rho)(l_4 - 2\rho)}{(m_{2,4} + 4\rho)^2}| \leq .004699575268$ by Proposition 2.42.

Thus $|\bar{E}_M(r, \theta) - \bar{E}_M(r_1, \theta_1)| \leq 3 \cdot .00002959264763 + 3 \cdot .003135336024 + 3 \cdot .004699575268 = .02359351182$.

The lowest energy of any of the 115996 boundary knots by Maple is 189.9216712. Recall that $\bar{E}_M(r_0, \theta_0) = 189.8741631 \leq 189.9216712 - .02359351182$. Thus every knot on the boundary of R has a higher energy than (r_0, θ_0) . This tells us that the dihedral six segment knots have a local minimum inside of the region R .

□

2.8 Finding a Critical Knot Conformation for E_M .

Theorem 2.44 (Fundamental Existence - Uniqueness Theorem). *Let U be an open subset of \mathbb{R}^n containing \mathbf{x}_0 and assume that $F \in C^1(U)$. Then there exists an $a > 0$ such that the initial value problem*

$$\dot{\mathbf{x}} = F(\mathbf{x})$$

$$\mathbf{x}(0) = \mathbf{x}_0$$

has a unique solution trajectory $\gamma(t, \mathbf{x}_0)$ on the interval $t \in [-\epsilon, \epsilon]$.

Lemma 2.45. *Let A be an orthogonal linear transformation on \mathbb{R}^{18} with the property that $\tilde{E}_M \circ A = \tilde{E}_M$. Then $(\nabla \tilde{E})(A(\mathbf{x})) = A((\nabla \tilde{E})(\mathbf{x}))$ for all $\mathbf{x} \in \mathbb{R}^{11}$.*

Proof.

$$\begin{aligned}
\tilde{E}_M(A(\mathbf{x})) &= \tilde{E}(\mathbf{x}) \\
\mathcal{D}(\tilde{E}_M \circ A)(\mathbf{x}) &= \mathcal{D}\tilde{E}_M(\mathbf{x}) \\
\mathcal{D}\tilde{E}_M(A(\mathbf{x})) \cdot A(\mathbf{x}) &= \mathcal{D}\tilde{E}_M(\mathbf{x}) \\
(A(\mathbf{x}))^T \cdot (\mathcal{D}\tilde{E}_M(A(\mathbf{x})))^T &= (\mathcal{D}\tilde{E}_M(\mathbf{x}))^T \\
(A(\mathbf{x}))^{-1} \cdot \nabla\tilde{E}_M(A(\mathbf{x})) &= \nabla\tilde{E}_M(\mathbf{x}) \\
\nabla\tilde{E}_M(A(\mathbf{x})) &= A(\mathbf{x}) \cdot \nabla\tilde{E}_M(\mathbf{x})
\end{aligned}$$

□

Let $\mathbf{x} \in D \cap \tilde{\mathcal{K}}$ be regarded as a six segment dihedral knot in \mathbb{R}^3 . Then there is a group of orthogonal linear transformations of \mathbb{R}^{18} corresponding to rotations of in \mathbb{R}^3 , that cyclically permute the vertices of \mathbf{x} . Let A be one of these rotations. Let P_A be the permutation map on \mathbb{R}^{18} associated to A .

Define the vector field \mathcal{X} on $\tilde{\mathcal{K}}$ by $\mathcal{X}(\mathbf{x}) = -(\nabla\tilde{E}_M)(\mathbf{x})$. By the Fundamental Theorem of ODE's, for \mathcal{X} there is a unique trajectory $\gamma(t, \mathbf{x}_0)$ for $\epsilon \leq t \leq \epsilon$ that passes through $\mathbf{x}_0 = \gamma(0, \mathbf{x}_0) = f(r_0, \theta_0)$. The trajectory satisfies $\gamma'(t, \mathbf{x}_0) = -(\nabla\tilde{E}_M)(\gamma(t, \mathbf{x}_0))$ for $\epsilon \leq t \leq \epsilon$.

Proposition 2.46. *Every point in the trajectory $\gamma(t, \mathbf{x}_0)$ is a dihedral knot.*

Proof. Since $f(r_0, \theta_0)$ is a dihedral knot, there is a group G six rotations A_1, \dots, A_6 that cyclically permute its vertices. Let P_{A_i} be the permutation map on \mathbb{R}^{18} associated to A_i . Then $A_i(f(r_0, \theta_0)) = P_{A_i}(f(r_0, \theta_0))$ for all i .

Consider the path $A_i(\gamma(t, \mathbf{x}_0))$, $\epsilon \leq t \leq \epsilon$. We can see that $\gamma'(t, \mathbf{x}_0) = -(\nabla\tilde{E}_M)(\gamma(t, \mathbf{x}_0))$ implies that

$$A_i(\gamma'(t, \mathbf{x}_0)) = A_i(-(\nabla\tilde{E}_M)(\gamma(t, \mathbf{x}_0))) = -(\nabla\tilde{E}_M)(A_i(\gamma(t, \mathbf{x}_0))),$$

by the lemma. This means that $A_i(\gamma(t, \mathbf{x}_0))$, $\epsilon \leq t \leq \epsilon$ must be the unique trajectory of \mathcal{X} passing through $A_i(\gamma(0, \mathbf{x}_0))$. Similarly, the path $P_{A_i}(\gamma(t, \mathbf{x}_0))$, $\epsilon \leq t \leq \epsilon$ is also the unique trajectory of \mathcal{X} passing through $P_{A_i}(\gamma(0, \mathbf{x}_0)) = A_i(\gamma(0, \mathbf{x}_0))$. Thus $P_{A_i}(\gamma(t, \mathbf{x}_0)) = A_i(\gamma(t, \mathbf{x}_0))$ for $\epsilon \leq t \leq \epsilon$. Thus every knot in $\gamma(t, \mathbf{x}_0)$ is dihedral.

Corollary 2.47 (From Perko, [9]). *Let U be an open subset of \mathbb{R}^n containing \mathbf{x}_0 . Let $F \in C^1(U)$ and let $[0, \beta)$ be the right maximal interval of existence of the solution $\mathbf{x}(t)$ of the initial value problem,*

$$\dot{\mathbf{x}} = F(\mathbf{x}), \quad \mathbf{x}(0) = \mathbf{x}_0$$

Assume that there is a compact set $R \subset U$ such that

$$\{\mathbf{y} \in \mathbb{R}^n \mid \mathbf{y} = \mathbf{x}(t) \text{ for some } t \in [0, \beta)\} \subset R.$$

Then it follows that $\beta = \infty$; i. e. the initial value problem has a solution $\mathbf{x}(t)$ on $[0, \infty)$.

Proposition 2.48. *The trajectory $\gamma(t, \mathbf{x}_0)$ is defined for $t \geq 0$ and is contained in $h_{18}^{-1}(R) \cap \tilde{\mathcal{K}}$.*

Proof. The path $h_{18}(\gamma(t, \mathbf{x}_0))$ is well defined by Proposition 2.46 . Since

$$\bar{E}_M(h_{18}(\gamma(t_1, \mathbf{x}_0))) \geq \bar{E}_M(h_{18}(\gamma(t_2, \mathbf{x}_0)))$$

for $t_1 < t_2$, the path $h_{18}(\gamma(t, \mathbf{x}_0))$ must remain inside of the region R . By Corollary 2.47, $\gamma(t, \mathbf{x}_0)$ is defined for $t \geq 0$ □

Proposition 2.49. *The set $h_{18}^{-1}(R) \cap \tilde{\mathcal{K}}$ in \mathbb{R}^{18} is compact.*

Proof. We will show that $h_{18}^{-1}(R) \cap \tilde{\mathcal{K}}$ is closed and bounded and thus, by the Bolzano Weierstrass Theorem, is compact.

- $h_{18}^{-1}(R) \cap \tilde{\mathcal{K}}$ *closed:* The set $h_{18}^{-1}(R) \cap \tilde{\mathcal{K}}$ is closed because h_{18} is continuous, R is a closed set in \mathbb{R}^2 , and $\tilde{\mathcal{K}}$ is closed.
- $h_{18}^{-1}(R) \cap \tilde{\mathcal{K}}$ *bounded:* We will show that $h_{18}^{-1}(R) \cap \tilde{\mathcal{K}}$ is contained in a bounded set. For any $\tilde{\mathbf{x}} \in D$ the segments $\tilde{S}_1(\tilde{\mathbf{x}})$, $\tilde{S}_3(\tilde{\mathbf{x}})$, and $\tilde{S}_5(\tilde{\mathbf{x}})$ are longer than the segments $\tilde{S}_2(\tilde{\mathbf{x}})$, $\tilde{S}_4(\tilde{\mathbf{x}})$, and $\tilde{S}_6(\tilde{\mathbf{x}})$. Since $\tilde{S}_1(\tilde{\mathbf{x}})$, $\tilde{S}_3(\tilde{\mathbf{x}})$, and $\tilde{S}_5(\tilde{\mathbf{x}})$ are all length 1, the point $\tilde{\mathbf{x}}$ can be no further than 6 units from the origin. Thus D is bounded. Since $h_{18}^{-1}(R) \cap \tilde{\mathcal{K}} \subset D$, the set $h_{18}^{-1}(R) \cap \tilde{\mathcal{K}}$ must also be bounded.

Thus $h_{18}^{-1}(R) \cap \tilde{\mathcal{K}}$ is compact. □

Also, since the function f is continuous on R and R is compact in \mathbb{R}^2 , the image $f(R)$ must be compact in \mathbb{R}^{18} .

For the following definition and theorems, let \mathcal{X} be the vector field of the system $\dot{\mathbf{x}} = f(\mathbf{x})$, where $f \in C^1(U)$ and U is an open subset of \mathbb{R}^n .

Definition 2.50 ([9]). *A point $\mathbf{p} \in U$ is an ω -limit point of the trajectory $\Gamma = \gamma(\cdot, \mathbf{x})$ of the system $\dot{\mathbf{x}} = f(\mathbf{x})$ if there is a sequence $t_n \rightarrow \infty$ such that*

$$\lim_{n \rightarrow \infty} \phi(t_n, \mathbf{x}) = \mathbf{p}.$$

The set of all limit points of Γ is $\omega(\Gamma)$.

Theorem 2.51 ([9]). *Let Γ be a trajectory in \mathcal{X} . Then $\omega(\Gamma)$ is a closed subset of U and if Γ is contained in a compact subset of \mathbb{R}^n , then $\omega(\Gamma)$ is a non-empty, connected compact subset of U .*

Theorem 2.52 ([13]). *Consider a vector field \mathcal{X} corresponding to $\dot{\mathbf{x}} = -\nabla V(\mathbf{x})$ for $\mathbf{x} \in \mathbb{R}^n$, where $V(\mathbf{x})$ is a scalar valued function on \mathbb{R}^n . Suppose that \mathbf{x}_0 is an ω -limit point of a trajectory of \mathcal{X} . Then \mathbf{x}_0 is a fixed point of \mathcal{X} .*

Let U be the interior of $h_{18}^{-1}(R) \cap \tilde{\mathcal{K}}$. Consider trajectory $\gamma(\cdot, \mathbf{x}_0)$ where $\mathbf{x}_0 = f(r_0, \theta_0)$. Then by Theorem 2.51 the ω -limit set $\omega(\gamma(\cdot, \mathbf{x}_0))$ is a nonempty subset of U . Let $\mathbf{p} \in \omega(\gamma(\cdot, \mathbf{x}_0))$. Because $h_{18}^{-1}(R) \cap \tilde{\mathcal{K}}$ is closed, $\mathbf{p} \in h_{18}^{-1}(R) \cap \tilde{\mathcal{K}}$. By Theorem 2.52, \mathbf{p} is a fixed point solution of the system $\dot{\mathbf{x}} = -\nabla \tilde{E}_M(\mathbf{x})$, and therefore a critical point of \tilde{E}_M .

Theorem 2.53. *Let \mathbf{p} be defined as above. Then for all $\mathbf{x} \in g^{-1}(\mathbf{p})$, \mathbf{x} is a critical point of E_M .*

Proof. By definition, $\nabla \tilde{E}_M(\mathbf{p}) = 0$. Since $(\tilde{E}_M \circ g)(\mathbf{x}) = E(\mathbf{x})$, then $D(\tilde{E}_M \circ g)(\mathbf{x}) = D\tilde{E}_M(g(\mathbf{x})) \cdot Dg(\mathbf{x}) = DE_M(\mathbf{x})$. But $D\tilde{E}_M(g(\mathbf{x})) = D\tilde{E}_M(\mathbf{p}) = \mathbf{0}$. Then $DE_M(\mathbf{x}) = 0$.

□

2.9 Future Work

I suspect, and would like to prove, that \mathbf{p} is a local minimum. I also could envision trying find critical knot for the minimum distance energy in other knot types.

CHAPTER 3

COMPLEMENTARY DOMAINS OF ARRANGEMENTS

In this chapter, we investigate a question of general geometric interest that was inspired by the article “Möbius Transformations of Polygons and Partitions of 3 - space.” A space \mathbb{R}^n can be separated into components by codimension 1 hypersurfaces. The number of components created depends on how the collection of hypersurfaces intersect each other. It would be convenient to have an upper bound to the number of components, given the number and algebraic degree of the surfaces. So far, we can supply an upper bound for algebraic curves in \mathbb{R}^2 and ellipsoids in \mathbb{R}^3 .

Definition 3.1. *We define a **domain** to be an open connected subset of \mathbb{R}^n .*

3.1 Origin of the Problem

In 2008, Richard Randell, Jonathan Simon, and Joshua Tokle published the article “Möbius Transformations of Polygons and Partitions of 3-space” in the **Journal of Knot Theory and its Ramifications** [10]. A portion of this article is spent explaining that, given a polygonal knot, many knot types can be represented as a spherical inversion of said knot. Spherical inversion does not map segments to segments. While the inversion of a polygon is not polygonal, we may simply invert the set of vertices of the polygon and consider the new polygon that the image of these vertices will make after the inversion. We call this process polygonal inversion.

Any four points in \mathbb{R}^3 are contained by a unique two-sphere (or plane). Given m points in \mathbb{R}^3 , consider the collection of $\binom{m}{4}$ spheres created by them. This collection of spheres divides \mathbb{R}^3 into a number of complementary domains.

Let P be an m -segment polygonal knot embedded in \mathbb{R}^3 . Let $\{S_1, \dots, S_n\}$ be

the collection of spheres associated to the vertices of P . Let ρ_0 and ρ_1 be polygonal inversions with radius of inversion 1 and centers at points c_0 and c_1 . (We will refer to the polygon created by connecting the images of the vertices of P after the inversion ρ by $\rho(P)$.) Let $\alpha(t)$ be a path from $\alpha(0) = c_0$ to $\alpha(1) = c_1$ that misses P . This path gives us a homotopy H_t of polygonal inversions, which gives us a homotopy of inverted polygons $H_t(P)$, where $H_t(P)$ is the image of polygonal knot P under a polygonal inversion of radius 1 centered at $\alpha(t)$. Notice that $H_0 = \rho_0$ and $H_1 = \rho_1$. If $\rho_0(P)$ and $\rho_1(P)$ are two different knot types, there must have been a point $\alpha(t_0)$ in the path α when the knot $H_{t_0}(P)$ is self-intersecting. Let E and F be two non-adjacent edges of the knot $H_{t_0}(P)$ that intersect. Let the endpoints of E and F be $H_{t_0}(w)$, $H_{t_0}(x)$, $H_{t_0}(y)$, and $H_{t_0}(z)$. Since E and F intersect, they must be coplanar, thus the vertices $H_{t_0}(x)$, $H_{t_0}(y)$, and $H_{t_0}(z)$ must also be coplanar. Then the points w , x , y , and z must lie on a sphere along with the center of inversion.

As long as the path α is contained within one of the complementary domains of the collection $\{S_1, \dots, S_n\}$ then all of the polygonal knots in the homotopy $H_t(P)$ have the same knot type. If the centers c_1 and c_2 of polygonal inversions ρ_1 and ρ_2 share the same complementary domain, then $\rho_1(P)$ and $\rho_2(P)$ have the same knot type. Thus the number of knot types that polygonal knot P can achieve through polygonal inversion can be bounded above by the number of complementary domains of $\{S_1, \dots, S_n\}$.

So the question remains: Given a collection of n spheres in \mathbb{R}^3 , how many complementary domains are there? Counting the number of complementary domains isn't a trivial task. The article [10] uses the following geometric argument to place an upper bound on the number of complementary domains of a collection of spheres.

Any pair of spheres must intersect in a circle, a single point, or not at all. The following proposition will be useful.

Proposition 3.2. *Let $\{C_1, \dots, C_k\}$ be a collection of circles in the sphere S . Then the complement of $S \setminus \cup C_i$ has at most $k^2 - k + 2$ components.*

Proof: The proof will proceed by induction. The $k = 1$ case is true. Assume true for $k-1$ circles. A new circle C_k intersects the other $k - 1$ circles in at most $2(k - 1)$ points. This divides C_k into at most $2(k - 1)$ arcs. Each arc may create at new path component. Then k circles divides S into

$$[(k - 1)^2 - (k - 1) + 2] + 2(k - 1) = k^2 - k + 2$$

components. □

The proof of the desired theorem proceeds in much the same way.

Theorem 3.3. *Let $\{S_1, \dots, S_n\}$ be any collection of two-spheres in \mathbb{R}^3 . Then $\mathbb{R}^3 \setminus \cup_{i=1}^n S_i$ has at most*

$$\frac{n^3}{3} - n^2 + \frac{8n}{3} = 2 \binom{n}{3} + 2n$$

components.

Proof: This proof will also proceed by induction. The $n = 1$ case is true. Assume it holds for $n - 1$ spheres. The new sphere S_n will intersect each of the $n - 1$ spheres in at most a single circle. Thus the union $\cup_{i=1}^{n-1} S_i$ divides the sphere S_n into at most $(n - 1)^2 - (n - 1) + 2$ regions. Each region of S_n creates at most one new domain in \mathbb{R}^3 . Thus the number of components in $\mathbb{R}^3 \setminus \cup_{i=1}^n S_i$ is

$$\frac{(n - 1)^3}{3} - (n - 1)^2 + \frac{8(n - 1)}{3} + (n - 1)^2 - (n - 1) + 2 = \frac{n^3}{3} - n^2 + \frac{8n}{3} \quad \square$$

3.2 Intersection Lattices and Homology

In 1993, Gunter Ziegler and Rade Živaljević published an article, *Homotopy Types of Subspace Arrangements via Diagrams of Spaces*, which contains a technique that we would like to use to investigate how arrangements of hypersurfaces can

separate \mathbb{R}^2 or \mathbb{R}^3 . Their method constructs an order complex from the intersection poset of the subspaces used in the arrangement. We can determine the number of complementary domains of the arrangement via the homology of the order complex and through Alexander Duality.

Let $\mathcal{A} = \{A_1, \dots, A_n\}$ be a finite collection of subspaces of \mathbb{R}^n so that \mathcal{A} is closed under intersection and each A_i is a finite disjoint union of topological balls and spheres of any dimension less than n .

Corresponding to the collection \mathcal{A} of subspaces is a poset $\mathcal{P} = \{p_1, \dots, p_n\}$. Each element A_i of \mathcal{A} corresponds to the element p_i in \mathcal{P} . The partial ordering on the set \mathcal{P} is given by reversed inclusion. We would say that $p_i \leq p_j$ exactly when $A_j \subseteq A_i$.

From here we create the order complex $\Delta(\mathcal{P})$ of the poset \mathcal{P} . Let each element of \mathcal{P} be a vertex of $\Delta(\mathcal{P})$. The simplices in $\Delta(\mathcal{P})$ correspond to ordered linear chains. The maximal element in the complex corresponds to the empty set and is denoted by $\hat{1}$. Define $\mathcal{P}_{<p}$ to be the subposet of elements of \mathcal{P} less than p .

Theorem 3.4 ([14]). *Define $d(p)$ to be the geometric dimension of the subspace associated to the poset element p . Let \mathcal{A} be a collection of topological spheres embedded in \mathbb{R}^n with the properties defined above. Let \mathcal{P} be the corresponding intersection poset. Then the following isomorphism holds by Alexander Duality.*

$$\tilde{H}^i(\mathbb{R}^n \setminus \cup_j A_j) \cong \bigoplus_{p \in \mathcal{P}, d(p) \neq 0} \tilde{H}_{n-d(p)-i-2}(\Delta(\mathcal{P}_{<p})).$$

If \mathcal{A} is a collection of spheres embedded in S^n , the n -sphere, with the properties defined above, then the following isomorphism holds.

$$\tilde{H}^i(S^n \setminus \cup_j A_j) \cong \bigoplus_{p \in \mathcal{P}, d(p) \neq 0} \tilde{H}_{n-d(p)-i-2}(\Delta(\mathcal{P}_{<p})).$$

Example. Consider ellipsoids E_1 , E_2 , and E_3 . Let $E_1 \cap E_2$ be a pair of curves C_{12} and D_{12} . Let $E_1 \cap E_3$ in a single curve C_{13} and let $E_2 \cap E_3$ be a pair of curves C_{23} and D_{23} . Let $C_{12} \cap C_{13} \cap C_{23}$ be a pair of points a and b . Let

$D_{12} \cap C_{13} \cap D_{23}$ be a pair of points c and d . For simplicity's sake, we will name the elements of \mathcal{P} by using the names of their corresponding subspace in \mathcal{A} . Then $\mathcal{P} = \{E_1, E_2, E_3, C_{12}, D_{12}, C_{13}, C_{23}, D_{23}, a, b, c, d, \hat{1}\}$. The order complex $\Delta(\mathcal{P})$ is shown in Figure 3.1.

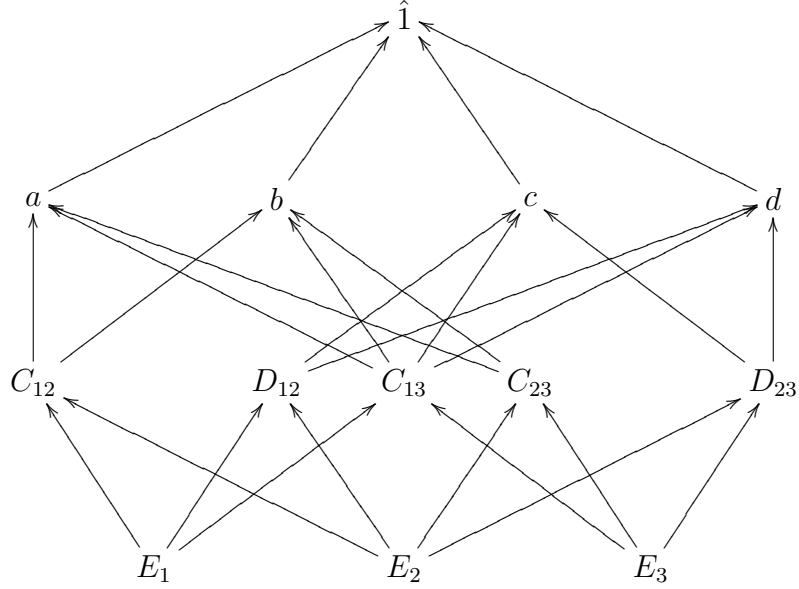


Figure 3.1: Complex for ellipsoid example.

Let's find $\tilde{H}^0(\mathbb{R}^3 \setminus (E_1 \cup E_2 \cup E_3))$. Since

$$\{p \in \mathcal{P} \mid d(p) \neq 0\} = \{E_1, E_2, E_3, C_{12}, D_{12}, C_{13}, C_{23}, D_{23}, \hat{1}\}$$

We have the following contributions to homology:

- $\tilde{H}_{-1}(\Delta(\mathcal{P}_{<E_1})) \cong \tilde{H}_{-1}(\Delta(\mathcal{P}_{<E_2})) \cong \tilde{H}_{-1}(\Delta(\mathcal{P}_{<E_3})) \cong \tilde{H}_{-1}(\emptyset) \cong \mathbb{Z}$ (It is convention that $\tilde{H}_{-1}(\emptyset) \cong \mathbb{Z}$.)
- $\tilde{H}_0(\Delta(\mathcal{P}_{<C_{12}})) \cong \tilde{H}_0(\Delta(\mathcal{P}_{<D_{12}})) \cong \tilde{H}_0(\Delta(\mathcal{P}_{<C_{13}})) \cong \tilde{H}_0(\Delta(\mathcal{P}_{<C_{23}}))$
 $\cong \tilde{H}_0(\Delta(\mathcal{P}_{<D_{23}})) \cong \mathbb{Z}$ because the subcomplexes $\Delta(\mathcal{P}_{<C_{12}})$, $\Delta(\mathcal{P}_{<D_{12}})$, $\Delta(\mathcal{P}_{<C_{13}})$, $\Delta(\mathcal{P}_{<C_{23}})$, $\Delta(\mathcal{P}_{<D_{23}})$ all consist of two vertices without an edge in between them.
- $\tilde{H}_2(\Delta(\mathcal{P}_{<\hat{1}})) = \mathbb{Z}^2$. This is less obvious than previous contributions. The

subcomplex $\Delta(\{a, C_{12}, C_{13}, C_{23}, E_1, E_2, E_3\})$ forms a disc, call it D_a with a at the center and the remaining elements at the edge. The points $b, c,$ and d all form corresponding discs: $D_b, D_c,$ and D_d . We can now see that $D_a \cup D_b$ and $D_c \cup D_d$ are spheres.

This means that $\tilde{H}^0(\mathbb{R}^3 \setminus \cup_i A_i) \cong \bigoplus_{p \in \mathcal{P}, d(p) \neq 0} \tilde{H}_{1-d(p)}(\Delta(\mathcal{P}_{<p})) \cong \mathbb{Z}^{10}$. The number of complementary domains must be 11.

With these tools we can find the number of complementary domains of any arrangement of $(n-1)$ - spheres as long as we can construct the intersection poset. Using geometry we can determine how collections of ellipsoids might intersect.

3.3 Bezout's Theorem

Throughout this paper, Bezout's Theorem will be invaluable to us as it give us an upper bound on the number of points of intersection between algebraic surfaces.

Theorem 3.5 (Bezout's Theorem, [11]). *The number of solutions in $\mathbb{C}\mathbb{P}^n$ of a system of n homogeneous equations in $n + 1$ unknowns is either infinite or equal to the product of their degrees, provided solutions are counted with multiplicities.*

Corollary 3.6. *Let f_1 and f_2 be two algebraic curves of degree d_1 and d_2 in \mathbb{R}^2 . If their intersection is finite, then f_1 and f_2 intersect in at most $d_1 \cdot d_2$ points.*

3.4 General Position

Definition 3.7. *Let Y and Z be two submanifolds of differentiable manifold X . We say the Y and Z intersect transversely at $x \in Y \cap Z$ if $T_x(Y) + T_x(Z) = T_x(X)$.*

Definition 3.8. *We will say that an arrangement of algebraic curves C_1, \dots, C_n is in general position if:*

1. *Every intersection between two curves C_i and C_j is a transversal intersection.*
2. *No point in any of the curves is in the intersection of three or more curves.*

Definition 3.9. *We will say that an arrangement of algebraic surfaces $\Sigma_1, \dots, \Sigma_n$ is in general position if:*

1. *If surfaces Σ_i and Σ_j intersect, then they do so transversely.*
2. *If Σ_i, Σ_j and Σ_k are surfaces so that $\Sigma_i \cap \Sigma_j \cap \Sigma_k \neq \emptyset$, then the manifolds $\Sigma_i \cap \Sigma_j$ and Σ_k intersect transversely everywhere in the intersection.*

3.5 Complementary Domains of Algebraic Curves.

We have a very nice upper bound for the number of intersections of algebraic curves in Theorem 3.6. We can use this with Theorem 3.4 to give us an upper bound to the number of complementary domains of an arrangement of algebraic curves.

The theorem will be easier to explain if we first show the use of Theorem 3.4 in an example of an arrangement of algebraic curves.

Example:

Let E_1, E_2 , and E_3 be ellipses with $E_1 \cap E_2$ being four points a, b, c , and d . Let $E_1 \cap E_3$ be a pair of points e and f . Let $E_2 \cap E_3$ be empty.

Then this arrangement of ellipses has the following order complex.

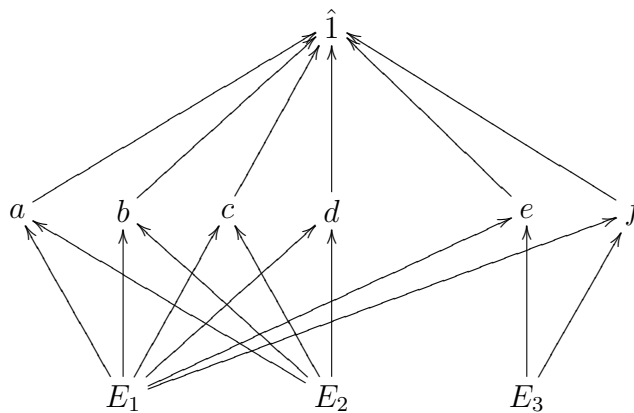


Figure 3.2: Complex for ellipse example

For each $p \in \mathcal{P}$ corresponding to an ellipse, $\tilde{H}_{-1}(\Delta(\mathcal{P}_{<p})) \cong \tilde{H}_{-1}(\emptyset) \cong \mathbb{Z}$ (by

convention).

We also see that $\Delta(\mathcal{P}_{<\hat{i}})$ is the following subcomplex.

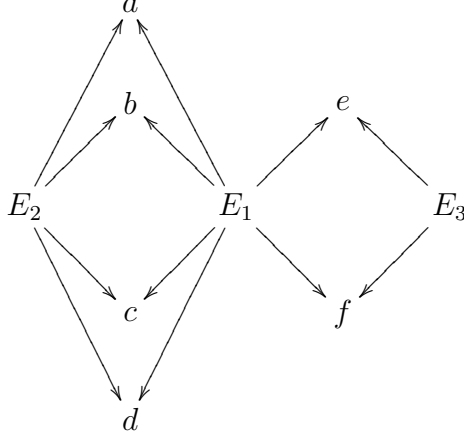


Figure 3.3: The subcomplex $\Delta(\mathcal{P}_{<\hat{i}})$ for ellipse example.

Thus $\tilde{H}_1(\Delta(\mathcal{P}_{<\hat{i}})) \cong \mathbb{Z}^4$. Then $\tilde{H}^0(\mathbb{R}^2 \setminus \cup E_i) \cong \mathbb{Z}^7$. This means that $\mathbb{R}^2 \setminus \cup E_i$ has eight domains.

Let C_1, \dots, C_n be a collection of algebraic curves that are homotopy equivalent to the circle S^1 and embedded in \mathbb{R}^2 with degrees at most d . Let the curves be in general position. In order to find the number of complementary domains to an arrangement of we need to know the number of ellipses and the 1-homology of the complex $(\Delta(\mathcal{P}_{<\hat{i}}))$.

Definition 3.10 ([6]). Let Δ be a complex with highest dimension n . Let α_k be the number of k -cells in the complex Δ . We define the **Euler Characteristic** $\chi(\Delta)$ to be $\chi(\Delta) = \sum_{i=0}^n (-1)^i \alpha_i$.

Definition 3.11 ([6]). If the group $H_q(X)$ is finitely generated, then we define $\beta_q = \text{rank}(H_q(X))$ to be the **q 'th betti number** of X .

Theorem 3.12 ([6]). If Δ is a finite complex of dimension n on the X , then the Euler Characteristic satisfies the following equation: $\chi(\Delta) = \sum_{i=0}^n (-1)^i \beta_i$.

Definition 3.13. Let $B_r(\mathbf{x}) \subset \mathbb{R}^n$ be the ball of radius r around $\mathbf{x} \in \mathbb{R}^n$. Let $\bar{B}_r(\mathbf{x})$ be the closure of $B_r(\mathbf{x})$.

Definition 3.14. Let $\pi_2 : \mathbb{R}^2 \longrightarrow \mathbb{S}^2$ be stereographic projection of the plane into \mathbb{S}^2 . Denote the point at infinity by $\{\infty\}$. Let $U_i = \mathbb{S}^2 \setminus \bar{B}_i(0)$ for $i \in \mathbb{Z}_{>0}$. If τ is the standard topology on \mathbb{R}^2 , let the topology on \mathbb{S}^2 be

$$\pi_2(\tau) \cup \{U_i\}_{i \in \mathbb{Z}_{>0}}.$$

Definition 3.15. Let M_f be a dimension 1 submanifold of \mathbb{R}^2 . Let C_1, \dots, C_s be the connected components of M_f . Let C_1, \dots, C_r for $r \leq s$ be bounded components of M_f . Define $C_1^+, \dots, C_r^+ \in \mathbb{S}^2$ by $C_i^+ = \pi_2(C_i)$. Let C_{r+1}, \dots, C_s be unbounded components of M_f . Define $C_{r+1}^+, \dots, C_s^+ \in \mathbb{S}^2$ by $C_i^+ = \pi_2(C_i) \cup \infty$.

Lemma 3.16. The components C_1^+, \dots, C_s^+ are all homeomorphic to the circle \mathbb{S}^1 .

Proof. The components C_1, \dots, C_r are all compact 1-manifolds. The map π_2 is continuous, so C_1^+, \dots, C_r^+ are also compact 1-manifolds, making them homeomorphic to the circle. Let $\bigcup V_\alpha$ be a collection of open sets that covers C_j^+ for $r+1 \leq j \leq s$. One U_i must be in the set. But $C_j^+ \setminus U_i = \pi_2(C_j \cap \bar{B}_i(0))$, which is compact. So C_j^+ is a compact 1-manifold as well. \square

Definition 3.17. Let $f(x, y) : \mathbb{R}^2 \longrightarrow \mathbb{R}$ be a smooth function with regular value 0. Define $M_f = \{(x, y) | f(x, y) = 0\}$.

Theorem 3.18. Let $f_1(x, y), \dots, f_n(x, y)$ be a collection of polynomials of degree d or less and having 0 as a regular value. Let M_{f_1}, \dots, M_{f_n} intersect each other generally and let $M_{f_1} \cup \dots \cup M_{f_n}$ be connected. Let C_1, \dots, C_s where $s \geq n$ be the collection of all of the connected components of M_{f_1}, \dots, M_{f_n} . Let r be the number of bounded components. Then,

- If C_1, \dots, C_s has s or $s - 1$ bounded curves, then $d^2 \binom{n}{2} + 2$ is an upper bound to the number of domains of $\mathbb{R}^2 \setminus \{M_{f_i}\}_{i=1}^n$.
- If C_1, \dots, C_s has r bounded curves where $r \leq s - 2$, then $d^2 \binom{n}{2} + (s - r) + 1$

is an upper bound to the number of domains of $\mathbb{R}^2 \setminus \{M_{f_i}\}_{i=1}^n$.

Proof. Instead of working with curves C_1, \dots, C_s in \mathbb{R}^2 , let us instead consider C_1^+, \dots, C_s^+ as an arrangement in \mathbb{S}^2 . Let $\Delta(\mathcal{P})$ be the order complex associated to C_1^+, \dots, C_s^+ . According to Theorem 3.4, we only need to consider the number of curves s in the arrangement and $H_1(\Delta(\mathcal{P}_{< \hat{i}}))$ in order to know $\tilde{H}^0(\mathcal{S}^2 \setminus \cup C_i^+)$.

There are at most $\binom{n}{2}$ ways to choose pairs of manifolds to intersect. Bezout's theorem (Theorem 3.6) says that the number of points in the intersection of M_{f_i} and M_{f_j} is at most d^2 distinct points. This means that C_i^+ and C_j^+ intersect at $\{\infty\}$ if both unbounded and at a maximum of d^2 other points. Each of these points adds another vertex to $\Delta(\mathcal{P}_{< \hat{i}})$. By Theorem 3.12, $b_1 = e - v + 1$ where b_1 is the first betti number of $\Delta(\mathcal{P}_{< \hat{i}})$ and e and v are the numbers of vertices and edges in the complex respectively. Then we can maximize b_1 by ensuring that $e - v$ is as large as possible.

If C_i is bounded, the vertex in $\Delta(\mathcal{P}_{< \hat{i}})$ representing the curve C_i^+ is adjacent only to the vertices associated with points of intersection (none of them $\{\infty\}$) between C_i^+ and some other curve. Each point of intersection between curves adds one vertex and two edges to the complex, thereby increasing $e - v$ by one. Thus each bounded curve can add at most d^2 to $e - v$.

If C_i is unbounded then the curve intersect the point $\{\infty\}$. If there is any other unbounded curve, then $\{\infty\}$ is a point of intersection. In this case, each unbounded curve adds one edge to the complex (between itself and $\{\infty\}$) as well as possibly adding d^2 to $e - v$.

Then if C_1, \dots, C_s has one or zero unbounded curves,

$$\begin{aligned} e - v &\leq \{\text{edges between curves and points of intersection}\} \\ &\quad - \{\text{vertices from point of intersection}\} \\ &\quad - \{\text{vertices from curves}\}. \end{aligned}$$

Then,

$$\tilde{b}_1 \leq d^2 \binom{n}{2} - s + 1$$

If C_1, \dots, C_s has $s - r$ unbounded curves where $s - r \geq 2$,

$$\begin{aligned} e - v &\leq \{\text{edges between curves and points of intersection}\} \\ &+ \{\text{edges between curves and } \infty\} \\ &- \{\text{vertices from point of intersection}\} \\ &- \{\text{vertices from curves}\} \\ &- \{\text{vertex for } \infty\}. \end{aligned}$$

Then

$$\tilde{b}_1 \leq d^2 \binom{n}{2} - r.$$

When we include the homology that we get from the the curves themselves, we find that if C_1, \dots, C_s has one or zero unbounded curves then,

$$\begin{aligned} \text{rank}(\tilde{H}^0(\mathbb{S}^2 \setminus \cup_i C_i^+)) &= \{\sum_{d(p)=1} b_{-1}(\Delta(\mathcal{P}_{<p}))\} + b_1(\Delta(\mathcal{P}_{<1})) \\ &\leq s + d^2 \binom{n}{2} - s + 1 \\ &= d^2 \binom{n}{2} + 1. \end{aligned}$$

If C_1, \dots, C_s has $s - r$ unbounded curves where $s - r \geq 2$ then,

$$\begin{aligned} \text{rank}(\tilde{H}^0(\mathbb{S}^2 \setminus \cup_i C_i^+)) &= \{\sum_{d(p)=1} \tilde{b}_{-1}(\Delta(\mathcal{P}_{<p}))\} + \tilde{b}_1(\Delta(\mathcal{P}_{<1})) \\ &\leq s + d^2 \binom{n}{2} - r \\ &= d^2 \binom{n}{2} + (s - r). \end{aligned}$$

Then the number of domains in $\mathbb{S}^2 \setminus \cup_i C_i^+$ (and thus $\mathbb{R}^2 \setminus \cup_i C_i$) is less than $d^2 \binom{n}{2} + 2$ if C_1, \dots, C_s has one or zero unbounded curves. And the number of domains is less than $d^2 \binom{n}{2} + (s - r) + 1$ if C_1, \dots, C_s has $s - r$ unbounded curves where $s - r \geq 2$.

□

3.6 Complementary Domains of Ellipsoids

Expanding the above theorem into three dimensions is considerably more difficult. In particular, it is difficult to understand how many curves of intersection there may be between the surfaces, even when given the degree. For this reason, we are restricting ourselves to degree 2, compact, non-degenerate algebraic surfaces: ellipsoids.

Definition 3.19. We define the **centroid** of a smooth space curve $\begin{bmatrix} x(t) \\ y(t) \\ z(t) \end{bmatrix}$, $a \leq$

$t \leq b$ in \mathbb{R}^3 to be the point $(\bar{x}, \bar{y}, \bar{z})$, where

$$\bar{x} = \frac{1}{b-a} \int_a^b x(t) dt$$

$$\bar{y} = \frac{1}{b-a} \int_a^b y(t) dt$$

and,

$$\bar{z} = \frac{1}{b-a} \int_a^b z(t) dt$$

Note that the centroid translates and rotates with the space curve through any rigid motion.

Lemma 3.20. Let C be a smooth closed curve in \mathbb{R}^3 . Let P be a plane through the centroid of C . Then there are at least two distinct points in $P \cap C$.

Proof: Without loss of generality, we may assume that the centroid c of C is located at the origin. We may also assume that P is the xy-plane. There are cases:

- If C lies entirely within P , then there are infinitely many points of C that lie in P and we are done.
- If C lies entirely above P (meaning that $z(t) > 0$), then $\bar{z} > 0$. This cannot be.
- If C lies entirely below P (meaning that $z(t) < 0$), then $\bar{z} < 0$. This also cannot be.

- If $z(t) > 0$ for some t -values and $z(t) < 0$ for some t -values, then there are at least two points of C that must lie in P , by the intermediate value theorem.

Lemma 3.21. *Let C_1, C_2 and C_3 be three smooth simple closed curves individually embedded in \mathbb{R}^3 . Then there is a plane P intersecting $C_1 \cup C_2 \cup C_3$ in six or more points.*

Proof. Let c_1, c_2 , and c_3 , be the centroids for C_1, C_2 and C_3 . Let P be the plane through c_1, c_2 , and c_3 . Then by Lemma 3.20, P intersects $C_1 \cup C_2 \cup C_3$ in six or more points. \square

Lemma 3.22. *Let E_1, E_2 be ellipsoids embedded in \mathbb{R}^3 . Then there are no more than two curves of intersection between E_1 and E_2 .*

Proof. Assume that there are at least 3 curves of intersection between Σ_1 and Σ_2 . Consider three curves of intersection C_1, C_2 and C_3 . By Lemma 3.21 there is a plane P that intersects $C_1 \cup C_2 \cup C_3$ in six or more points. The intersections $\Sigma_1 \cap P$ and $\Sigma_2 \cap P$ (both degree 2 (or lower) planar curves) must have at least six points in common then. By Bezout's theorem, the maximal number of points in the intersection $\Sigma_1 \cap \Sigma_2 \cap P$ is four. This is a contradiction. Thus there are two or fewer curves of intersection between Σ_1 and Σ_2 . \square

Theorem 3.23. *Let E_1, \dots, E_n be a collection of ellipsoids in general position.*

Then $\mathbb{R}^3 \setminus E_i$ has, at most,

$$\frac{4n^3}{3} - 3n^2 + \frac{8n}{3} + 1$$

domains.

Proof. Let $d(p) = 2$. Then p is associated with a surface E_i in \mathcal{A} . Then

$$\tilde{H}_{-1}(\Delta(\mathcal{P}_{<p})) = \tilde{H}_{-1}(\emptyset) = \mathbb{Z}.$$

Thus $\sum_{d(p)=2} \tilde{b}_{-1}(\Delta(\mathcal{P}_{<p})) = n$

Let $d(p) = 1$. Then p is associated with a curve of intersection C_{ij} between surfaces S_i and S_j . Then $\tilde{H}_0(\Delta(\mathcal{P}_{<p})) = \mathbb{Z}$ because $\Delta(\mathcal{P}_{<p})$ consists of the pair of

points associated to S_i and S_j . By Lemma 3.22, the maximum number of curves of intersection in the intersection poset is $2\binom{n}{2} = n(n-1)$. Then $\sum_{d(p)=1} \tilde{b}_0(\Delta(\mathcal{P}_{<p})) \leq n(n-1)$.

Let $p = \hat{1}$. We will now try to understand the structure of the complex $\Delta(\mathcal{P}_{<\hat{1}})$. Consider the subcomplex created by all p in the poset where $d(p) = 1, 2$. There are no 2 cells in this subcomplex. Consider all of the vertices adjacent to the the element associated to a point of triple intersection a . We will say that a is in the intersection $\Sigma_i \cap \Sigma_j \cap \Sigma_k$ and that it is contained in curves of intersection C_{ij} , C_{ik} , and C_{jk} . The point a must be contained in three distinct curves because it is contained in $\Sigma_i \cap \Sigma_j$, $\Sigma_i \cap \Sigma_k$, and $\Sigma_j \cap \Sigma_k$. Thus, the vertex corresponding to a is adjacent to six other vertices in $\Delta(\mathcal{P}_{<\hat{1}})$, namely the vertices corresponding to Σ_i , Σ_j , Σ_k , C_{ij} , C_{ik} , and C_{jk} . The vertex corresponding to Σ_i is adjacent to the vertices corresponding to C_{ij} and C_{ik} . A similar statement can be made of the vertices corresponding to the other ellipsoids and curves. We see that the vertex corresponding to a must be in the center of a hexagon D_a in the order complex $\Delta(\mathcal{P}_{<\hat{1}})$.

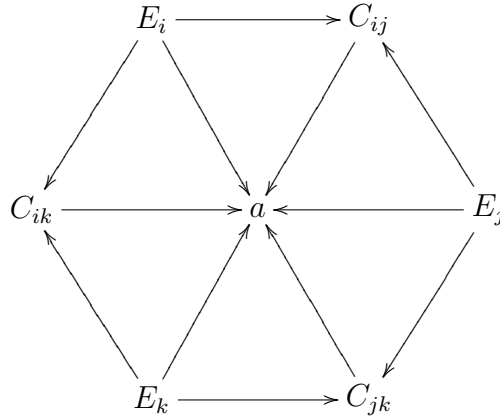


Figure 3.4: The hexagon D_a .

All 2-cells in the complex $\Delta(\mathcal{P}_{<\hat{1}})$ are pieces of a hexagon like the one above.

This hexagon D_a only shares the entire boundary with hexagon D_q when point of triple intersection q is contained in $\Sigma_i \cap \Sigma_j \cap \Sigma_k$ and $C_i \cap C_j \cap C_k$. The complex gains 2-homology if this is the case. Each point of triple intersection adds a disk to the complex, which has the potential of adding a rank to $\tilde{H}_2(\Delta(\mathcal{P}_{<1}))$. By Bezout's Theorem 3.5, there are a maximum of 8 points of triple intersection between any three ellipsoids. Thus $\tilde{b}_2(\Delta(\mathcal{P}_{<1})) \leq 8\binom{n}{3} = (\frac{4}{3})(n^3 - 3n^2 + 2n)$.

Thus

$$\begin{aligned} \text{rank}(\tilde{H}^0(\mathbb{R}^3 \setminus \bigcup E_i)) &= \sum_{d(p)=2} \tilde{b}_{-1}(\Delta(\mathcal{P}_{<p})) + \sum_{d(p)=1} \tilde{b}_0(\Delta(\mathcal{P}_{<p})) + \tilde{b}_2(\Delta(\mathcal{P}_{<1})) \\ &\leq n + n(n-1) + (\frac{4}{3})(n^3 - 3n^2 + 2n) \\ &= \frac{4n^3}{3} - 3n^2 + \frac{8n}{3} \end{aligned}$$

Then the number of domains in $\mathbb{R}^3 \setminus \bigcup E_i$ is less than or equal to $\frac{4n^3}{3} - 3n^2 + \frac{8n}{3} + 1$.

□

3.7 Future Work

The upper bounds that I have reported seem to be sharp for lower numbers of hypersurfaces of lower degrees. I would like to find out the circumstances under which this upper bound is sharp.

I would also like to find an upper bound for more arrangements of surfaces in \mathbb{R}^3 . The greatest difficulty right now is placing an upper bound on the number of curves of intersection of any two surfaces.

CHAPTER 4

INSCRIBED POLYGONS UNDER ARCLENGTH PRESERVING ISOTOPIES

4.1 Definitions

Throughout the course of this paper we will refer to a curve \mathbb{C} in \mathbb{R}^3 . For our purposes, \mathbb{C} is a closed, simple, regular, and C^2 -smooth.

Definition 4.1. A curve is said to be regular if it has a parametrization $\alpha(t)$ for which $\alpha'(t)$ is nonzero for all t .

Definition 4.2. If \mathbb{C} is a closed simple regular, smooth curve embedded in \mathbb{R}^3 , define $scsd(\mathbb{C}) = \min\{d(x, y) \mid (x, y) \in \mathbb{C} \times \mathbb{C} \text{ where } (y - x) \perp T_x\}$

Definition 4.3. If \mathbb{C} is a closed simple regular, smooth curve embedded in \mathbb{R}^3 , define $dcsd(\mathbb{C}) = \min\{d(x, y) \mid (x, y) \in \mathbb{C} \times \mathbb{C} \text{ where } (y - x) \perp T_x \text{ and } (y - x) \perp T_y\}$.

Definition 4.4. Let \mathbb{C} be a regular curve with unit speed parametrization $\alpha : I \rightarrow \mathbb{R}^3$. Let $\kappa(t)$ be the curvature at $\alpha(t) \in C$. If $\kappa_m = \sup\{\kappa(t) \mid t \in I\}$ then we define $R_K(C) = 1/\kappa_m$ to be the minimum radius of curvature.

Definition 4.5. If \mathbb{C} is a closed simple regular, smooth curve embedded in \mathbb{R}^3 , define $R_A = \frac{1}{2}dcsd(\mathbb{C})$.

Definition 4.6. Let \mathbb{C} be a closed simple regular, smooth curve embedded in \mathbb{R}^3 with parametrization $\alpha(t)$. Let $E = \{(\alpha(t), v) \in C \times \mathbb{R}^3 \mid \alpha'(t) \cdot v = 0\}$. Define $\exp : E \rightarrow \mathbb{R}^3$ by $\exp(x, v) = x + v$. Define $\bar{E}_r = \{(x, v) \in E \mid \|v\| \leq r\}$. Finally, define $R_I = \sup\{r \mid \exp \text{ is injective on } \bar{E}_r\}$.

Definition 4.7. Define the ropelength of knot K by $ropelength(K) = \frac{arclength(K)}{R_I(K)}$.

Theorem 4.8 ([5]). For any smooth, simple, closed, regular curve $R_I = \min\{R_K, R_A\}$.

Definition 4.9. If $x, y \in \mathbb{C}$ then define $arc(x, y)$ to be the length of the shortest arc between x and y .

Theorem 4.10 (Schur, [3]). Let C be a plane arc with the curvature $\kappa(s)$ which

forms a convex curve with its chord AB . Let C^* be an arc of the same length referred to by the same parameter s such that its curvature $\kappa^*(s) \leq \kappa(s)$. If d^* and d denote the lengths of the chords joining their endpoints, then $d \leq d^*$. Moreover, the equality sign holds when and only when C and C^* are congruent.

4.2 Creating the Polygon

Lemma 4.11. *Let $x, y_1, y_2 \in \mathbb{C}$ so that $\|x - y_i\| \geq R_I$. Then every point y on the arc between y_1 and y_2 not containing x has the property $\|x - y\| \geq R_I$.*

Proof. Denote by α the arc between y_1 and y_2 not containing x . Let y^* be the closest point on α to x . (We are guaranteed one by EVT.) Then $(x - y^*) \perp T_{y^*}$. Then $\|x - y^*\| \geq 2scsd(\mathbb{C}) \geq 2R_I$. \square

Lemma 4.12. *For all $x, y \in \mathbb{C}$, $\|x - y\| < 2R_I \Rightarrow arc(x, y) \leq \pi R_I$.*

Proof. Let N be the normal plane to $x \in \mathbb{C}$. This plane must intersect \mathbb{C} in at least two places. WLOG we may assume that y is on or above the plane N .

1. *Case 1:* If $y \in N$ then $\|x - y\| \geq scsd(\mathbb{C}) \geq R_I$.
2. *Case 2:* If y is on the same arc (call it α) above N as x , then either $arc(x, y) \leq \pi R_I$ (we are done) or $arc(x, y) > \pi R_I$. If the latter, denote by z_1 the point on α with the property $arc(x, z_1) = \pi R_I$. By Schur's Theorem, $\|x - z_1\| \geq 2R_I$. Denote by z_2 the endpoint of α that is not x . Then $\|x - z_2\| \geq 2scsd(\mathbb{C}) \geq 2R_I$. By the previous lemma, $\|x - y\| \geq 2R_I$.
3. *Case 3:* Let y be a point on some other arc β above the plane N . Denote intersection points of $\beta \cup P$ by z_1 and z_2 . Then $\|x - z_i\| \geq scsd(\mathbb{C}) \geq R_I$, which by the previous lemma implies that $\|x - y\| \geq R_I$.

□

Let Σ be a 2-sphere of radius $r \leq R_K$.

Lemma 4.13. *Let \mathbb{C}_0 , an arc of \mathbb{C} , have the following properties:*

- \mathbb{C}_0 has one of its endpoints c_0 on Σ .
- At c_0 , \mathbb{C} is tangent to Σ .
- The arclength of \mathbb{C}_0 is πR_K or less.

Then \mathbb{C}_0 intersects Σ at some other point only if $r = R$ and \mathbb{C}_0 is an arc of a great circle on Σ .

Proof. For simplicity's sake, let Σ be centered at the origin. Assume that \mathbb{C}_0 also intersects Σ at its other endpoint c_1 . (WLOG We assume there are no other points of intersection.) Let A be an arc of a great circle on Σ starting at c_0 , in the direction of c_1 , and of the same length as \mathbb{C}_0 . Call the endpoints of A by c_0 and a_1 . There are two cases:

1. $c_1 \in A$: In this case, the length of the chord between c_0 and c_1 is shorter than or equal to the length of the chord between c_0 and a_1 . If the chord is shorter, then we are in contradiction to Schur's Theorem. If the chords is of equal length, then there are two cases:
 - (a) $r < R_K$, which also contradicts Schur's Theorem.
 - (b) $r = R_K$, which by Schur's Theorem implies that A and \mathbb{C}_0 are congruent, ensuring that \mathbb{C}_0 is an arc of a great circle of Σ .
2. $c_1 \notin A$: Let $A_0 \supset A$ be the arc on Σ from c_0 to c_1 . Note that the arclength of A_0 is greater than the arclength of \mathbb{C}_0 . Consider the projection $\pi : \mathbb{R}^3 \rightarrow \Sigma$ defined by $\pi(\rho, \theta, \phi) = (r, \theta, \phi)$, written in spherical coordinates. This is an arclength decreasing projection as \mathbb{C}_0 is disjoint from the interior of Σ . As

$\pi(\mathbb{C}_0)$ is a curve on Σ from c_0 to c_1 , it must have arclength greater than or equal to that of A_0 , the shortest curve on Σ from c_0 to c_1 . Thus $length(A_0) > length(\mathbb{C}_0) \geq length(\pi(\mathbb{C}_0)) \geq length(A_0)$, a contradiction. \square

Let S be a chord between two points of \mathbb{C} .

Definition 4.14. Let T_C to be the tube around \mathbb{C} created by taking the union of the open normal disks of radius ρ around every point of \mathbb{C} .

Definition 4.15. Let T_S to be the tube around S created by taking the union of the open normal disks of radius ρ around every point of S .

Lemma 4.16. The chord S separates \mathbb{C} into two arcs. If S is not contained in T_C , then in each arc there is a point c that is:

1. On a plane normal to S at some point $s \in S$, and
2. Outside of T_S .

Proof. WLOG choose one of the two arcs. Call this arc \mathbb{C}_S . Let $s \in S$ be a point outside of T_C . Let $\tilde{c} \in \mathbb{C}$ be the closest point in \mathbb{C} to s . Although $(\tilde{c} - s) \perp T_{\tilde{c}}\mathbb{C}$, $s \notin T_C$ guarantees that $\|\tilde{c} - s\| > \rho$. Because \mathbb{C}_S and S share endpoints, \mathbb{C}_S must intersect the plane normal to S at s . Call the closest of these points of intersection c . But $\|c - s\| > \|\tilde{c} - s\| > \rho$. Thus c is outside of T_S . \square

Definition 4.17. Any chord S between two points of \mathbb{C} divides \mathbb{C} into two arcs. We will say that the shortest arc of \mathbb{C} is spanned by S and refer to the length of said arc as the span of S .

Let $\rho \in [0, R_I)$.

Proposition 4.18. If $span(S) < 2R_K[\arccos(1 - \frac{\rho}{R_K})]$ then $S \subset T_C$.

Proof. Let \mathbb{C}_s be the arc of \mathbb{C} spanned by S . Say that S is not contained in T_C . Then by Lemma 4.16, there is a point \tilde{c} of \mathbb{C}_S on a plane normal to S at some point

$s \in S$ and not contained in T_S . Let L be the line that is identified by S . Then there is some point \tilde{c} of \mathbb{C}_S on a plane normal to L and not contained in the ρ -tube T_L around L . Of the points of \mathbb{C}_S with these properties, find the point c_0 that is farthest from L . Call the point of L on the plane normal to L and intersecting c_0 by l . Consider the 2-sphere Σ with:

1. radius R_K ,
2. center lying on the ray from c_0 through l , and
3. tangent to \mathbb{C}_S at c_0 .

Consider one of the arcs of \mathbb{C}_S from c_0 to S . We will call this arc \mathbb{C}_0 and denote its endpoints c_0 and c_1 . It is sufficient to show that the length of \mathbb{C}_0 is greater than $R_K[\arccos(1 - \frac{\rho}{R_K})]$. By Lemma 4.13, \mathbb{C}_0 is either outside the sphere or it has arclength greater than $\frac{\pi R}{2} > R_K[\arccos(1 - \frac{\rho}{R_K})]$. Recall the projection $\pi : \mathbb{R}^3 \rightarrow \Sigma$. If \mathbb{C}_0 lies outside the sphere, then its length must be longer than the shortest curve in the sphere connecting c_0 and $\pi(c_1)$. Call this curve A_0 . If $length(A_0) > \frac{\pi R_K}{2}$ then we are done. If $length(A_0) \leq \frac{\pi R_K}{2}$, then L intersects A_0 by some easy geometry. By simple geometric argument, the length of the shortest arc from c_0 to the point where L intersects A_0 is $R_K[\arccos(1 - \frac{\rho}{R_K})] < length(A_0) < length(\mathbb{C}_0)$. Since this argument applies to both arcs in \mathbb{C}_S from c_0 to S , we know that $length(\mathbb{C}_S) = span(S) \geq 2R_K[\arccos(1 - \frac{\rho}{R_K})]$. \square

Any polygon inscribed in \mathbb{C} and composed of chords with spans less than $2R_K[\arccos(1 - \frac{\rho}{R_K})]$ will be contained in the T_C of \mathbb{C} . We will place the vertices of a polygon P so that the spans of the segments of P are equal to each other. The polygon P will be inside T_C as long as the number of vertices is larger than $\frac{arclength(\mathbb{C})}{2R_K[\arccos(1 - \frac{\rho}{R_K})]}$.

Lemma 4.19. *Let P be a polygon inscribed in \mathbb{C} such that each segment of P has a span that is strictly less than $2R_K[\arccos(1 - \frac{\rho}{R_K})]$. Further let the vertices of P ,*

v_1 through v_n , be arranged in a cyclic order around \mathbb{C} . Then P is isomorphic to \mathbb{C} .

Proof. Show that P intersects any normal disk transversally.

Let D be a ρ -disk centered at $c_0 \in \mathbb{C}$ and normal to \mathbb{C} with S a segment of P that is intersecting it. We will show that S and D cannot lie in the same plane. By way of contradiction, assume S and D are coplanar. First, S cannot be contained entirely within D . If it were, then there would be at least two points of \mathbb{C} inside of D , namely, the endpoints of S . Thus one of the endpoints of S must be outside of D . Then S must intersect ∂D at some point p . Consider a sphere Σ with radius ρ centered at p . If \mathbb{C} intersects Σ at no point other than c_0 , then p is not close enough to \mathbb{C} to be in T_C , which contradicts Proposition 4.18. Let c_1 be another point of \mathbb{C} that intersects Σ . Then $\|c_0 - c_1\| \leq 2\rho$. There are two cases:

1. $\|c_0 - c_1\| < 2\rho$: By Lemma 4.12, $\text{arc}(c_0, c_1) \leq \pi R_I \leq \pi R_K$. But by Lemma 4.13 either $\rho = R_K$, which contradicts hypothesis, or $\text{arc}(c_0, c_1) > \pi R_K$.
2. $\|c_0 - c_1\| = 2\rho$ (i.e. c_0 and c_1 are antipodal points on Σ): If \mathbb{C} is tangent to the sphere Σ at c_1 , then p is not close enough to \mathbb{C} to be in T_C . If \mathbb{C} crosses into the interior of Σ at c_1 , then \mathbb{C} must also intersect Σ at some other point c_2 to exit the sphere. This is impossible, by the previous case.

Thus any normal disks of T_C that are intersected by a segment of P are intersected transversally.

Show that every disk is intersected by P at least once.

Let D be a normal ρ -disk that intersects \mathbb{C} at c_0 . Let Π be the plane containing D . If c_0 is a vertex we are done. Then c_0 is between some vertices v_i and $v_i + 1$ of P . The vertices v_i and $v_i + 1$ separate \mathbb{C} into two arcs. Let the arc containing c_0 be called \mathbb{C}_0 . Let S be the segment between v_i and $v_i + 1$. Let \mathbb{C}_S be the arc of \mathbb{C} spanned by S . There are two possibilities:

1. *Both v_i and $v_i + 1$ lie on one side of Π* : Since \mathbb{C}_0 intersects Π orthogonally,

the length of \mathbb{C}_0 must be at least $\pi R_K \geq 2R_K[\arccos(1 - \frac{\rho}{R_K})]$. Then there must be some vertex of P on \mathbb{C}_0 . But then c_0 is not between v_i and $v_i + 1$.

2. *Vertices v_i and $v_i + 1$ lie on opposite sides of Π :* Let $s \in S$ be arbitrary. Let Σ be a sphere of radius ρ centered at s . If Σ contains no point of \mathbb{C}_S , then \mathbb{C}_S is longer than $2R_K[\arccos(1 - \frac{\rho}{R_K})]$. Thus every point of S is no further than ρ from some point of \mathbb{C}_S . In other words, $S \subseteq \cup_{c \in \mathbb{C}_S} B(c, \rho)$, where $B(c, \rho)$ is a *rho*-ball around c . The disk D separates $\cup_{c \in \mathbb{C}_S} B(c, \rho)$ into two components, so S must intersect D .

Show that P may intersect each normal ρ -disk exactly once. Let D be a disk that has non-trivial intersection with segments S_i , with endpoints v_i and $v_i + 1$, and S_j with endpoints v_j and $v_j + 1$. WLOG let $i < i + 1 < j < j + 1$. If both S_i and S_j intersect D , then the vertices $v_i, v_i + 1, v_j$, and $v_j + 1$ cannot be in cyclic ordering, contradicting the hypothesis.

Since P intersects each ρ -disk of T_C exactly once, we may use the isotopy in Milnor's "On the Curvature of Knots" [7] to isotope P onto \mathbb{C} .

□

4.3 Arclength Preserving Isotopies

Let $f : [0, L) \longrightarrow \mathbb{R}^3$ be an arclength parametrization of \mathbb{C} .

Definition 4.20. *We say that $F : S^1 \times I \longrightarrow \mathbb{R}^3$ is an arclength preserving isotopy if:*

1. F is an isotopy of S^1 embedded in \mathbb{R}^3 .
2. $\text{arc}(F(s_1, i), F(s_2, i))$ is, for any $s_1, s_2 \in S^1$, constant over all $i \in I$.

Let $F : S^1 \times I \longrightarrow \mathbb{R}^3$ be an arclength preserving isotopy. We will refer to the knot parametrized by $F(s, t_0)$ as K_{t_0} .

Definition 4.21. *Let the radius of curvature of K_{t_0} be denoted by R_{K, t_0} and the supremum injectivity radius of K_{t_0} by R_{I, t_0} .*

Let $\rho_{t_0} \in [0, R_{I,t_0})$ for each $t_0 \in [0, L)$. Let T_{t_0} be the ρ_{t_0} -tube around K_{t_0} .

Let K_0 and K_1 be two knots isotopic to each other by an arclength preserving isotopy. Let $\tilde{R} < \min_{t \in [0, L)} R_{K,t}$ and $\tilde{\rho} < \min_{t \in [0, L)} \rho_t$.

Consider a polygon P_0 inscribed in K_0 such that:

1. Each segment of P_0 has a span that is strictly less than $2\tilde{R}[\arccos(1 - \frac{\tilde{\rho}}{\tilde{R}})]$.
2. The vertices $v_{1,0} \dots v_{n,0}$ of P satisfy: Given $v_{i,0} = F(a, 0)$ and $v_{j,0} = F(b, 0)$, $i < j$ iff $a < b$.

Define P_t inscribed in K_t by letting $v_{i,t} = F(a, t)$ if $v_{i,0} = F(a, 0)$.

Theorem 4.22. *For all $t \in [0, L)$, $P_t \subset T_t$ and P_t is isotopic to K_t .*

Proof. Consider $v_{i,t} = F(a, t)$ and $v_{i+1,t} = F(b, t)$. Then

$$\arccos(\frac{v_{i,t} \cdot v_{i+1,t}}{|v_{i,t}| |v_{i+1,t}|}) = \arccos(\frac{F(a,t) \cdot F(b,t)}{|F(a,t)| |F(b,t)|}) = \arccos(\frac{F(a,0) \cdot F(b,0)}{|F(a,0)| |F(b,0)|}) < 2\tilde{R}[\arccos(1 - \frac{\tilde{\rho}}{\tilde{R}})].$$

Thus by Proposition 4.18, the segment of P_t connecting $v_{i,t}$ and $v_{i+1,t}$ is contained inside of T_t . This is, of course, true for all segments of P_t . Thus for every $t \in [0, 1]$ the polygon P_t is inscribed inside of K_t and remains within T_t . By Lemma 4.19, P_t is isotopic to K_t for every value of t .

□

4.4 Future Work

I would like to be able to find an arclength preserving isotopy of a knot K_0 into K_1 that forces the polygon P_t to intersect itself. This would indicate an isotopy that does not preserve the ropelength of K_0 . We define a thick isotopy to be an isotopy for which $\text{ropelength}(K_t) \leq \text{ropelength}(K_0)$ for all $0 \leq t \leq 1$. I would then like to find two knots K_1 and K_2 that are isotopy equivalent but not thick isotopy equivalent.

APPENDIX A

ENERGY MINIMIZATION EXPERIMENT

Note: It was necessary to add line breaks to the code in order to fit it to the page. The word “@@” before a line indicates that this line break wasn’t present in the code.

A.1 Gradient Descent Algorithm

```
import processing.opengl.*;
//Global Variables
int psi=0;
int theta=0;
int zm = 60;
float stepsize = .1;
int graddyn = -1;
int heatdyn = -1;
int showcoords = -1;
int showenergy = 1;

// These are the coordinates of the polygon that we are minimizing.
float[] [] vcs={{10,-10,0},{10*cos(7*PI/6),10,10*sin(7*PI/6)}
@@,{10*cos(2*PI/3),-10,10*sin(2*PI/3)},
@@{10*cos(11*PI/6),10,10*sin(11*PI/6)}
@@, {10*cos(4*PI/3),-10,10*sin(4*PI/3)}
@@,{10*cos(PI/2),10,10*sin(PI/2)}}};

void setup() {
  size(600,600,OPENGL);
  background(0);
  smooth();
  PFont font;
  font = loadFont("CourierNew-12.vlw");
  textFont(font);
  textSize(20);
  fill(200,200,00);
}

void draw() {
  background(0);
  strokeWeight(2);
```

```

stroke(180,0,0);
noFill();
camera(zm*cos(2*PI*-psi/600)*cos(2*PI*-theta/600)
@@,zm*sin(2*PI*-psi/600)*cos(2*PI*-theta/600)
@@,zm*sin(2*PI*-theta/600),0.0,0.0,0.0,0.0,1.0,0.0);

stroke(255,0,0);
line(0,0,0,5,0,0);
stroke(0,255,0);
line(0,0,0,0,5,0);
stroke(0,0,255);
line(0,0,0,0,0,5);
stroke(255);

//Centers the polygon
float[] avevcs = {0,0,0};
for (int i=0;i<3;i=i+1){
  for (int j=0; j<vcs.length; j=j+1){
    avevcs[i] = avevcs[i] + (vcs[j][i]/vcs.length);
  }
}
for (int i=0;i<vcs.length;i=i+1){
  for(int j=0; j<3;j=j+1){
    vcs[i][j] = vcs[i][j] - avevcs[j];
  }
}

if (graddyn == 1){
  //Makes temporary polygon
  float[][] vcstemp = new float[vcs.length][3];
  for (int i=0; i<vcs.length; i=i+1){
    for (int j=0; j<3; j=j+1) {
      vcstemp[i][j] = vcs[i][j];
    }
  }
  //Makes and uses the gradient
  float[] grad = {0,0,0};
  for (int i=0;i<vcs.length;i=i+1){
    for(int j=0; j<3;j=j+1){
      vcstemp[i][j] = vcstemp[i][j]+stepsize;
      grad[j] = MDEnergy(vcstemp)-MDEnergy(vcs);
      vcstemp[i][j] = vcs[i][j];
    }
  }
  float gradlength = sqrt(pow(grad[0],2)+pow(grad[1],2)
  @@+pow(grad[2],2));

  grad[0] = grad[0]*stepsize/gradlength;

```

```

grad[1] = grad[1]*stepsize/gradlength;
grad[2] = grad[2]*stepsize/gradlength;

for (int j = 0; j<3; j=j+1){
    vcs[i][j] = vcs[i][j]-grad[j];
}
}

}

if (heatdyn == 1){
    //Makes a random jitter set

    float[][] step = new float[vcs.length][3];
    for (int i=0; i<vcs.length;i=i+1){
        for (int j=0; j<3;j=j+1){
            step[i][j] = random(-stepsize,stepsize);
        }
    }

    float[][] vcstemp = new float[vcs.length][3];
    for (int i=0; i<vcs.length;i=i+1){
        for (int j=0;j<3;j=j+1){
            vcstemp[i][j] = vcs[i][j]+step[i][j];
        }
    }

    if(MDEnergy(vcstemp) < MDEnergy(vcs)){
        for (int i=0; i<vcs.length;i=i+1){
            for (int j=0;j<3;j=j+1){
                vcs[i][j] = vcstemp[i][j];
            }
        }
    }
}

//Draws the polygon
stroke(255);
beginShape();
for (int i=0; i< vcs.length; i=i+1) {
    vertex(vcs[i][0],vcs[i][1],vcs[i][2]);
}
endShape(CLOSE);

```

```

//Showing the coordinates of the vertices
if (showcoords ==1){

for (int i=0;i<vcs.length;i=i+1){
    textMode(MODEL);
    text("{"+round(vcs[i][0])+","+round(vcs[i][1])+","
        @@+round(vcs[i][2])+"}",vcs[i][0],vcs[i][1],vcs[i][2]);
}
}
//Show Energy
if (showenergy == 1){
    fill(255);
    textMode(SCREEN);
    text("MD Energy = " + MDEnergy(vcs),20,20);
}
}

void keyPressed() {
    if (key == 'w') {
        psi = psi+5;
    }
    if (key == 's') {
        psi = psi-5;
    }
    if (key == 'a') {
        theta = theta-5;
    }
    if (key == 'd') {
        theta = theta+5;
    }
    if (key == 'z') {
        zm = zm-1;
    }
    if (key == 'x') {
        zm = zm+1;
    }
    if (key == 'e') {
        showenergy = showenergy*(-1);
    }

    if (key == 'm') {
        stepsize = stepsize*4/3;
        println("stepsize =" + stepsize);
    }
    if (key == 'n') {
        stepsize = stepsize*.75;
    }
}

```

```

    println("stepsize =" + stepsize);
}
if (key == 'g') {
    graddyn = graddyn*(-1);
    println("toggle gradient dynamic");
}
if (key == 'h'){
    heatdyn = heatdyn*(-1);
    println("toggle heat dynamic");
}
if (key == 'v') {
    showcoords = showcoords*(-1);
}
if (key == 'o') {
    PrintWriter output;
    output = createWriter("outputknot.txt");
    for (int i=0;i<vcs.length;i=i+1){
        output.println("{"+vcs[i][0]+","+vcs[i][1]+","+vcs[i][2]+"}");
    }
    output.flush();
    output.close();
    println("saved to outputknot.txt");
}
}
}

```

A.2 Basic Functions

```

//Function that finds the length between two vertices
float vlen(float[] A, float[] B) {
    float res = sqrt(pow((A[0]-B[0]),2)+pow((A[1]-B[1]),2)
    @@+pow((A[2]-B[2]),2));
    return res;
}

//Dot product in 3 dimensions
float dot(float[] A, float[] B) {
    float res = A[0]*B[0]+A[1]*B[1]+A[2]*B[2];
    return res;
}

//Length of projection of A in the direction of B
float proj(float[] A,float[] B) {
    float res = dot(A,B)/dot(B,B);
    return res;
}

```

```

//Function outputs lengths between vertices
float[] alen(float[][] vcstemp){
    float[] res = new float[vcs.length];
    for (int m=0; m<vcs.length; m=m+1) {
        res[m] = vlen(vcstemp[(m+1)%vcs.length],vcstemp[m]);
    }
    return res;
}

//Function outputs unit direction vectors between vertices.
float[][] dir(float[][] vcstemp){
    float[][] res = new float[vcs.length][3];
    for (int k=0; k< 3; k=k+1) {
        for (int j=0; j<vcs.length; j=j+1) {
            res[j][k] =(vcstemp[(j+1) % vcs.length][k]-vcstemp[j][k])
                @@/(alen(vcstemp)[j]);
        }
    }
    return res;
}

```

A.3 Arclength

```

//Function for the arclength between two segments
float arclength(int r,int s,float[] alen) {
    float arc1 = 0;
    float arc2 = 0;
    if (r<s) {
        for (int i=0; i<r; i=i+1){
            arc1=arc1+alen[i];
        }
        for (int i=(s+1)%vcs.length;i<vcs.length; i=i+1){
            arc1=arc1+alen[i];
        }
        for (int i = r+1; i<s;i=i+1){
            arc2=arc2+alen[i];
        }
    }
    if (s < r) {
        for (int i=0; i<s; i=i+1){
            arc1=arc1+alen[i];
        }
        for (int i=(r+1)%vcs.length;i<vcs.length; i=i+1){
            arc1=arc1+alen[i];
        }
        for (int i = s+1; i<r;i=i+1){
            arc2=arc2+alen[i];
        }
    }
}

```



```

    }
}
float res = min(arc1,arc2);
return res;
}

```

A.4 Minimum Distance Function

```

//Find the distance between the given points on two segments.
float segdist(int r,int s,float tr,float ts ,float[] [] vcstemp){
float[] restemp1 = {vcstemp[r][0]+tr*dir(vcstemp)[r][0],vcstemp[r][1]
@@+tr*dir(vcstemp)[r][1],vcstemp[r][2]+tr*dir(vcstemp)[r][2]};
//println(restemp1);
float[] restemp2 = {vcstemp[s][0]+ts*dir(vcstemp)[s][0],vcstemp[s][1]
@@+ts*dir(vcstemp)[s][1],vcstemp[s][2]+ts*dir(vcstemp)[s][2]};
//println(restemp2);

float res = vlen(restemp1,restemp2);

return res;
}

```

```

//Function that finds the minimum distance between two edges
float md(int r,int s, float[] [] vcstemp) {

//Parameter of closest points if segments parallel and same direction.

float tr = 0;
float ts = 0;

if (dot(dir(vcstemp)[r],dir(vcstemp)[s])==1) {
//println("par");
if (proj(vcstemp[(r+1)%vcs.length],dir(vcstemp)[r])
@@<= proj(vcstemp[s],dir(vcstemp)[r])){
tr = alen(vcstemp)[r];
ts = 0;
}
else if (proj(vcstemp[(s+1)%vcs.length],dir(vcstemp)[r])
@@ <= proj(vcstemp[r],dir(vcstemp)[r])){
tr = 0;
ts = alen(vcstemp)[s];
}
else if (proj(vcstemp[r],dir(vcstemp)[r])
@@<= proj(vcstemp[s],dir(vcstemp)[r])){
tr = proj(vcstemp[s],dir(vcstemp)[r])
@@- proj(vcstemp[r],dir(vcstemp)[r]);
}
}

```

```

    ts = 0;
}
else if (proj(vcstemp[s],dir(vcstemp)[r])
@@<= proj(vcstemp[r],dir(vcstemp)[r])){
    tr = 0;
    ts = proj(vcstemp[r],dir(vcstemp)[r])
    @@- proj(vcstemp[s],dir(vcstemp)[r]);
}
return segdist(r,s,tr,ts,vcstemp);
}
//Parameter of closest points if segments parallel and
@@opposite direction.
else if (dot(dir(vcstemp)[r],dir(vcstemp)[s])==-1) {
    //println("opp");
    if (proj(vcstemp[(r+1)%vcs.length],dir(vcstemp)[r])
@@<= proj(vcstemp[(s+1)%vcs.length],dir(vcstemp)[r])){
        tr = alen(vcstemp)[r];
        ts = alen(vcstemp)[s];
    }
    else if (proj(vcstemp[s],dir(vcstemp)[r])
@@<= proj(vcstemp[r],dir(vcstemp)[r])){
        tr = 0;
        ts = 0;
    }
    else if (proj(vcstemp[r],dir(vcstemp)[r])
@@<= proj(vcstemp[(s+1)%vcs.length],dir(vcstemp)[r])){
        tr = proj(vcstemp[(s+1)%vcs.length],dir(vcstemp)[r])
        @@- proj(vcstemp[r],dir(vcstemp)[r]);
        ts = alen(vcstemp)[s];
    }
    else if (proj(vcstemp[(s+1)%vcs.length],dir(vcstemp)[r])
@@<= proj(vcstemp[r],dir(vcstemp)[r])){
        tr = 0;
        ts = alen(vcstemp)[s]-(proj(vcstemp[r],dir(vcstemp)[r])
        @@- proj(vcstemp[(s+1)%vcs.length],dir(vcstemp)[r]));
    }
}
return segdist(r,s,tr,ts,vcstemp);
}

//Parameter of closest points if segments are non-parallel.
else {
//println("not par");
float[] dottemp1 = {vcstemp[r][0]-vcstemp[s][0],vcstemp[r][1]
@@-vcstemp[s][1],vcstemp[r][2]-vcstemp[s][2]};
float[] dottemp2 = {vcstemp[s][0]-vcstemp[r][0],vcstemp[s][1]
@@-vcstemp[r][1],vcstemp[s][2]-vcstemp[r][2]};
float absr = (dot(dir(vcstemp)[r],dir(vcstemp)[s]))

```

```

    @@*dot(dir(vcstemp)[s],dottemp1)
    @+dot(dir(vcstemp)[r],dottemp2))
    @/(1-pow(dot(dir(vcstemp)[r],dir(vcstemp)[s]),2));
    float abss = (dot(dir(vcstemp)[r],dir(vcstemp)[s])
    @@*dot(dir(vcstemp)[r],dottemp2)
    @+dot(dir(vcstemp)[s],dottemp1))
    @/(1-pow(dot(dir(vcstemp)[r],dir(vcstemp)[s]),2));
    float s0 = constrain(-dot(dir(vcstemp)[s],dottemp2),0
    @,alen(vcstemp)[s]);
    float s1 = constrain(dot(dir(vcstemp)[r],dir(vcstemp)[s])
    @@*alen(vcstemp)[r] - dot(dir(vcstemp)[s],dottemp2)
    @,0,alen(vcstemp)[s]);
    float r0 = constrain(-dot(dir(vcstemp)[r],dottemp1)
    @,0,alen(vcstemp)[r]);
    float r1 = constrain(dot(dir(vcstemp)[r],dir(vcstemp)[s])
    @@*alen(vcstemp)[s]-dot(dir(vcstemp)[r],dottemp1)
    @,0,alen(vcstemp)[r]);

    if (0 <= absr && absr <= alen(vcstemp)[r] && 0
    @<= abss && abss <= alen(vcstemp)[s]){
        return segdist(r,s,absr,abss,vcstemp);
    }
    else {
        float[] minlist = {segdist(r,s,0,s0,vcstemp)
        @,segdist(r,s,alen(vcstemp)[r],s1,vcstemp)
        @,segdist(r,s,r0,0,vcstemp),segdist(r,s,r1
        @,alen(vcstemp)[s],vcstemp)};
        return min(minlist);
    }
}
}
}

//Finds the MD Energy of the the polygon
float MDEnergy(float[][] vcstemp) {

    float MDE = 0;
    for (int i = 0;i<vcs.length-2;i=i+1){
        for (int j = i+2; j<min(i+vcs.length-1,vcs.length);j=j+1){
            MDE = MDE + (alen(vcstemp)[i]*alen(vcstemp)[j])/(pow(md(i
            @,j,vcstemp),2));
            //println(dir(vcstemp)[i]);
            //println(dir(vcstemp)[j]);
            //println(i+" "+j+" "+(alen(vcstemp)[i]*alen(vcstemp)[j])
            @/(pow(md(i,j,vcstemp),2)));
        }
    }

    return MDE;
}

```

}

APPENDIX B

FINDING THE ENERGY ON THE BOUNDARY OF R

Note: It was necessary to add line breaks to the code in order to fit it to the page. The word “@@” before a line indicates that this line break wasn’t present in the code.

B.1 Maple Experiment

```

dot:=(a,b)->a[1]*b[1]+a[2]*b[2]+a[3]*b[3];
vect:=(a,b)-> [b[1]-a[1],b[2]-a[2],b[3]-a[3]];
dist:=(a,b)->sqrt((a[1]-b[1])^2+(a[2]-b[2])^2+(a[3]-b[3])^2);
vlength:=a->dist(a,[0,0,0]);
cross:=(a,b)->[a[2]*b[3]-a[3]*b[2],a[3]*b[1]-a[1]*b[3]
@@,a[1]*b[2]-a[2]*b[1]];
scalarmult:=(a,k)->[a[1]*k,a[2]*k,a[3]*k];
triple:=(a,b,c)->dot(a,cross(b,c));

a1:=(r,theta)->[1,-r,0];
a2:=(r,theta)->[cos(theta),r,sin(theta)];
a3:=(r,theta)->[-1/2,-r,sqrt(3)/2];
a4:=(r,theta)->[cos(theta+2*Pi/3),r,sin(theta+2*Pi/3)];
a5:=(r,theta)->[-1/2,-r,-sqrt(3)/2];
a6:=(r,theta)->[cos(theta+4*Pi/3),r,sin(theta+4*Pi/3)];

cvw:=(a,b,c,d,r,theta)->cross(vect(a(r,theta),b(r,theta))
@@,vect(c(r,theta),d(r,theta)));

segdist:=(a,b,c,d,r,theta)->abs(dot(a(r,theta)-c(r,theta)
@@,cvw(a,b,c,d,r,theta))/vlength(cvw(a,b,c,d,r,theta)));

dlength:=(r,theta)->sqrt(4*r^2+2-2*cos(theta));

ulength:=(r,theta)->sqrt(4*r^2+2+cos(theta)-sqrt(3)*sin(theta));

ddterm2:=(r,theta)->dlength(r,theta)^2/segdist(a1,a2,a3,a4,r,theta)^2;

duterm2:=(r,theta)->dlength(r,theta)*ulength(r,theta)
@@/(segdist(a1,a2,a4,a5,r,theta)^2);

```

```

uuterm2:=(r,theta)->ulength(r,theta)^2
@@/(segdist(a2,a3,a4,a5,r,theta)^2);
DMDE2:=(r,theta)->3*(ddterm2(r,theta)
@@+duterm2(r,theta)+uuterm2(r,theta));
DMDE2(r,theta);

r0 := .5261243504; theta0 := 4.642845642;

dlengthlist:=proc(epr,ept,dvr,dvt)
local i,res;
res=[];
for i from -dvr/2+1 to dvr/2 do;
res:=[op(res),[r0+2*i*epr/dvr,theta0+ept,evalf(dlength(r0+2*i*epr/dvr
@@,theta0+ept))]];
od;
for i from -dvr/2 to dvr/2-1 do;
res:=[op(res),[r0+2*i*epr/dvr,theta0-ept,evalf(dlength(r0+2*i*epr/dvr
@@,theta0-ept))]];
od;
for i from -dvt/2 to dvt/2-1 do;
res:=[op(res),[r0+epr,theta0+2*i*ept/dvt,evalf(dlength(r0+epr,theta0
@@+2*i*ept/dvt))]];
od;
for i from -dvt/2+1 to dvt/2 do;
res:=[op(res),[r0-epr,theta0+2*i*ept/dvt,evalf(dlength(r0-epr,theta0
@@+2*i*ept/dvt))]];
od;
res;
end proc;

ulengthlist:=proc(epr,ept,dvr,dvt)
local i,res;
res=[];
for i from -dvr/2+1 to dvr/2 do;
res:=[op(res),[r0+2*i*epr/dvr,theta0+ept,evalf(ulength(r0
@@+2*i*epr/dvr,theta0+ept))]];
od;
for i from -dvr/2 to dvr/2-1 do;
res:=[op(res),[r0+2*i*epr/dvr,theta0-ept,evalf(ulength(r0
@@+2*i*epr/dvr,theta0-ept))]];
od;
for i from -dvt/2 to dvt/2-1 do;
res:=[op(res),[r0+epr,theta0+2*i*ept/dvt,evalf(ulength(r0
@@+epr,theta0+2*i*ept/dvt))]];
od;

```

```

for i from -dvt/2+1 to dvt/2 do;
res:=[op(res), [r0-epr, theta0+2*i*ept/dvt, evalf(ulength(r0
@@-epr, theta0+2*i*ept/dvt))]];
od;
res;
end proc;

ddmd:=(r, theta)->segdist(a1, a2, a3, a4, r, theta);
ddmdlist:=proc(epr, ept, dvr, dvt)
local i, res;
res=[];
for i from -dvr/2+1 to dvr/2 do;
res:=[op(res), [r0+2*i*epr/dvr, theta0+ept, evalf(ddmd(r0
@@+2*i*epr/dvr, theta0+ept))]];
od;
for i from -dvr/2 to dvr/2-1 do;
res:=[op(res), [r0+2*i*epr/dvr, theta0-ept, evalf(ddmd(r0
@@+2*i*epr/dvr, theta0-ept))]];
od;
for i from -dvt/2 to dvt/2-1 do;
res:=[op(res), [r0+epr, theta0+2*i*ept/dvt, evalf(ddmd(r0
@@+epr, theta0+2*i*ept/dvt))]];
od;
for i from -dvt/2+1 to dvt/2 do;
res:=[op(res), [r0-epr, theta0+2*i*ept/dvt, evalf(ddmd(r0
@@-epr, theta0+2*i*ept/dvt))]];
od;
res;
end proc;

dumd:=(r, theta)->segdist(a1, a2, a4, a5, r, theta);
dumdlist:=proc(epr, ept, dvr, dvt)
local i, res;
res=[];
for i from -dvr/2+1 to dvr/2 do;
res:=[op(res), [r0+2*i*epr/dvr, theta0+ept, evalf(dumd(r0
@@+2*i*epr/dvr, theta0+ept))]];
od;
for i from -dvr/2 to dvr/2-1 do;
res:=[op(res), [r0+2*i*epr/dvr, theta0-ept, evalf(dumd(r0
@@+2*i*epr/dvr, theta0-ept))]];
od;
for i from -dvt/2 to dvt/2-1 do;
res:=[op(res), [r0+epr, theta0+2*i*ept/dvt, evalf(dumd(r0
@@+epr, theta0+2*i*ept/dvt))]];
od;
for i from -dvt/2+1 to dvt/2 do;
res:=[op(res), [r0-epr, theta0+2*i*ept/dvt, evalf(dumd(r0

```

```

@@-epr,theta0+2*i*ept/dvt))]];
od;
res;
end proc;
uumd:=(r,theta)->segdist(a2,a3,a4,a5,r,theta);
uumdlist:=proc(epr,ept,dvr,dvt)
local i,res;
res=[];
for i from -dvr/2+1 to dvr/2 do;
res:=[op(res),[r0+2*i*epr/dvr,theta0+ept,evalf(uumd(r0
@@+2*i*epr/dvr,theta0+ept))]];
od;
for i from -dvr/2 to dvr/2-1 do;
res:=[op(res),[r0+2*i*epr/dvr,theta0-ept,evalf(uumd(r0
@@+2*i*epr/dvr,theta0-ept))]];
od;
for i from -dvt/2 to dvt/2-1 do;
res:=[op(res),[r0+epr,theta0+2*i*ept/dvt,evalf(uumd(r0
@@+epr,theta0+2*i*ept/dvt))]];
od;
for i from -dvt/2+1 to dvt/2 do;
res:=[op(res),[r0-epr,theta0+2*i*ept/dvt,evalf(uumd(r0
@@-epr,theta0+2*i*ept/dvt))]];
od;
res;
end proc;
listmin:=proc(list,k)
local i,res ;
res=[];
for i from 1 to nops(list) do;
res:=[op(res),list[i][k]];
od;
min(res);
end proc;

listmax:=proc(list,k)
local i,res ;
res=[];
for i from 1 to nops(list) do;
res:=[op(res),list[i][k]];
od;
max(res);
end proc;

ddlist:=proc(epr,ept,dvr,dvt)
local i,res;
res=[];

```



```

for i from -dvr/2+1 to dvr/2 do;
res:=[op(res),[r0+2*i*epr/dvr,theta0+ept,evalf(ddterm2(r0
@@+2*i*epr/dvr,theta0+ept))]];
od;
for i from -dvr/2 to dvr/2-1 do;
res:=[op(res),[r0+2*i*epr/dvr,theta0-ept,evalf(ddterm2(r0
@@+2*i*epr/dvr,theta0-ept))]];
od;
for i from -dvt/2 to dvt/2-1 do;
res:=[op(res),[r0+epr,theta0+2*i*ept/dvt,evalf(ddterm2(r0
@@+epr,theta0+2*i*ept/dvt))]];
od;
for i from -dvt/2+1 to dvt/2 do;
res:=[op(res),[r0-epr,theta0+2*i*ept/dvt,evalf(ddterm2(r0
@@-epr,theta0+2*i*ept/dvt))]];
od;
res;
end proc;
dulist:=proc(epr,ept,dvr,dvt)
local i,res;
res=[];
for i from -dvr/2+1 to dvr/2 do;
res:=[op(res),[r0+2*i*epr/dvr,theta0+ept,evalf(duterm2(r0
@@+2*i*epr/dvr,theta0+ept))]];
od;
for i from -dvr/2 to dvr/2-1 do;
res:=[op(res),[r0+2*i*epr/dvr,theta0-ept,evalf(duterm2(r0
@@+2*i*epr/dvr,theta0-ept))]];
od;
for i from -dvt/2 to dvt/2-1 do;
res:=[op(res),[r0+epr,theta0+2*i*ept/dvt,evalf(duterm2(r0
@@+epr,theta0+2*i*ept/dvt))]];
od;
for i from -dvt/2+1 to dvt/2 do;
res:=[op(res),[r0-epr,theta0+2*i*ept/dvt,evalf(duterm2(r0
@@-epr,theta0+2*i*ept/dvt))]];
od;
res;
end proc;
uulist:=proc(epr,ept,dvr,dvt)
local i,res;
res=[];
for i from -dvr/2+1 to dvr/2 do;
res:=[op(res),[r0+2*i*epr/dvr,theta0+ept,evalf(uterm2(r0
@@+2*i*epr/dvr,theta0+ept))]];
od;
for i from -dvr/2 to dvr/2-1 do;

```

```

res:=[op(res),[r0+2*i*epr/dvr,theta0-ept,evalf(uuterm2(r0
@@+2*i*epr/dvr,theta0-ept))]];
od;
for i from -dvt/2 to dvt/2-1 do;
res:=[op(res),[r0+epr,theta0+2*i*ept/dvt,evalf(uuterm2(r0
@@+epr,theta0+2*i*ept/dvt))]];
od;
for i from -dvt/2+1 to dvt/2 do;
res:=[op(res),[r0-epr,theta0+2*i*ept/dvt,evalf(uuterm2(r0
@@-epr,theta0+2*i*ept/dvt))]];
od;
res;
end proc;

epr:=.01:
ept:=.01:
dvr:=29000:
dvt:=29000:

dllist:=dlengthlist(epr,ept,dvr,dvt):
dmin:=listmin(dllist,3);
dmax:=listmax(dllist,3);
save dmin, dmax, dhTemp;
ullist:=ulengthlist(epr,ept,dvr,dvt):
umin:=listmin(ullist,3);
umax:=listmax(ullist,3);
save umin,umax,dhTemp;
ddlist:=ddmdlist(epr,ept,dvr,dvt):
ddmin:=listmin(ddlist,3);
ddmax:=listmax(ddlist,3);
save ddmin,ddmax,dhTemp;
dulist:=dumdlist(epr,ept,dvr,dvt):
dumin:=listmin(dulist,3);
dumax:=listmax(dulist,3);
save dumin,dumax,dhTemp;
uulist:=uumdlist(epr,ept,dvr,dvt):
uumin:=listmin(uulist,3);
uumax:=listmax(uulist,3);
save uumin,uumax,dhTemp;
D2list:=[]:
for i from 1 to nops(dllist) do:
D2list:=[op(D2list),[dllist[i][1],dllist[i][2],3*(dllist[i][3]^2
@@/ddlist[i][3]^2+dllist[i][3]*ullist[i][3]/dulist[i][3]^2
@@+ullist[i][3]^2/uulist[i][3]^2)]];
od:

D2min:=listmin(D2list,3);

```

```
A:=[dmin,dmax,umin,umax,ddmin,ddmax,dumin,dumax,uumin,uumax,D2min];
```

```
save A,dhTemp;
```

```
quit;
```

REFERENCES

- [1] R. V. BUNYI AND T. W. KEPHART, *Glueballs and the universal energy spectrum of tight knots and links*, Int.J.Mod.Phys., A20 (2005), pp. 1252–1259.
- [2] P. D. L. R. G. D. C. WEBER, A. STASIAK, *Numerical simulation of gel electrophoresis of dna knots in weak and strong electric fields*, Biophysical Journal, 90 (2006), pp. 3100 – 3105.
- [3] S.-S. CHERN, *In Studies in Global Geometry and Analysis*, Prentice - Hall, 1967.
- [4] S. FUKUHARA, *Energy of a knot*, A Fete of Topology, (1988), pp. 443 – 461.
- [5] R. A. LITHERLAND, J. SIMON, O. DURUMERIC, AND E. RAWDON, *Thickness of knots*, Topology Appl., 91 (1999), pp. 233–244.
- [6] MASSEY, *A Basic Course in Algebraic Topology*, Springer, 1991.
- [7] J. W. MILNOR, *On the total curvature of knots*, Annals of Mathematics, 52 (1950), pp. 248 – 257.
- [8] J. O’HARA, *Energy of a knot*, Topology, 30 (1991), pp. 241–247.
- [9] L. PERKO, *Differential Equations and Dynamical Systems*, Springer - Verlag, 1991.
- [10] R. RANDELL, J. SIMON, AND J. TOKLE, *Mobius transformations of polygons and partitions of 3-space*, J. Knot Theory Ramifications, 17 (2008), pp. 1401–1413.
- [11] I. R. SHAFAREVICH, *Basic Algebraic Geometry*, Springer - Verlag, 1974.
- [12] J. K. SIMON, *Energy functions for polygonal knots*, J. Knot Theory Ramifications, 3 (1994), pp. 299–320. Random knotting and linking (Vancouver, BC, 1993).
- [13] S. WIGGINS, *Introduction to Applied Nonlinear Dynamical Systems and Chaos*, Springer, second ed., 1990.
- [14] G. M. ZIEGLER AND R. T. ŽIVALJEVIĆ, *Homotopy types of subspace arrangements via diagrams of spaces*, Math. Ann., 295 (1993), pp. 527–548.